

Exoplanet Biosignatures: A Framework for Their Assessment

David C. Catling^{1,2*}, Joshua Krissansen-Totton^{1,2}, Nancy Y. Kiang³, David Crisp⁴, Tyler D. Robinson⁵, Shiladitya DasSarma⁶, Andrew Rushby⁷, Anthony Del Genio⁸, William Bains⁹, Shawn Domagal-Goldman¹⁰.

¹Department of Earth and Space Sciences/Astrobiology Program, Box 351310, University of Washington, Seattle, WA 98103. ²Virtual Planetary Laboratory, University of Washington, Seattle. ³NASA Goddard Institute for Space Studies, 2880 Broadway, New York, NY 10025. ⁴MS 233-200, Jet Propulsion Laboratory, California Institute of Technology, 4800 Oak Grove Drive, Pasadena, CA 91109. ⁵Department of Astronomy and Astrophysics, University of California, Santa Cruz, CA 95064. ⁶Department of Microbiology and Immunology, School of Medicine, and Institute of Marine and Environmental Technology, University System of Maryland, Baltimore, Maryland 21202. ⁷NASA Ames Research Center, Moffett Field, CA 94035. ⁸NASA Goddard Institute for Space Studies, 2880 Broadway, New York, NY 10025. ⁹Department of Earth, Atmospheric and Planetary Science, MIT, 77 Mass. Ave., Cambridge, MA 02139. ¹⁰NASA Goddard Space Flight Center, Greenbelt, MD 20771.

*E-mail: dcatling@uw.edu

Abstract:

Finding life on exoplanets from telescopic observations is the ultimate goal of exoplanet science. Life produces gases and other substances, such as pigments, which can have distinct spectral or photometric signatures. Whether or not life is found in future data must be expressed with probabilities, requiring a framework for biosignature assessment. We present such a framework, which advocates using biogeochemical “Exo-Earth System” models to simulate potentially biogenic spectral or photometric data. Given actual observations, these simulations are then used to find the Bayesian likelihoods of those data occurring for scenarios with and without life. The latter includes “false positives” where abiotic sources mimic biosignatures. Prior knowledge of factors influencing inhabitation, including previous observations, is combined with the likelihoods to give the probability of life existing on a given exoplanet. Four components of observation and analysis are used. **1)** Characterization of stellar (e.g., age and spectrum) and exoplanetary system properties, including “external” exoplanet parameters (e.g., mass and radius) to determine its suitability for life. **2)** Characterization of “internal” exoplanet parameters (e.g., climate) to evaluate whether an exoplanet surface can host life. **3)** Assessment of potential biosignatures through environmental context (components 1-2) and corroborating evidence. **4)** Exclusion of false positives. The resulting Bayesian probabilities of life detection map to five confidence levels, ranging from “very likely” to “very unlikely” inhabited.

Keywords: Biosignatures; exoplanets; habitability; planetary science; Bayesian statistics; atmospheric composition

1. Introduction

In the future, if unusual combinations of gases or spectral features are detected on a potentially habitable exoplanet, consideration will undoubtedly be given to the possibility of their biogenic origin. But the extraordinary claim of life should be the hypothesis of last resort only after all conceivable abiotic alternatives are exhausted. This possibility of false positives – when a planet without life produces a spectral feature that mimics a biosignature – is one of the lessons we have learned from a thorough consideration of oxygen and ozone as biosignatures (Meadows et al., *this issue*). If life is suggested by remote data, the discovery will always have a degree of uncertainty and so the extent to which data suggest the presence of life should be assigned a probability. Following this self-critical scientific approach, we outline a general framework for detecting and verifying biosignatures in exoplanet observations. Research required to best implement this framework is discussed elsewhere (Walker et al., *this issue*), as are the missions and observatories that will eventually acquire the data (Fuji et al., *this issue*).

In its broadest definition, a *biosignature* is any substance, group of substances, or phenomenon that provides evidence of life (reviewed by Schwieterman et al., *this issue*). The objective of the framework described below is to identify the information and general procedure required to quantify and increase the confidence that a suspected biosignature detected on an exoplanet is truly a product of life.

2. A Bayesian framework for biosignature assessment and life detection

A Bayesian approach is an appropriate technique to provide a best-informed probability about a hypothesis when dealing with incomplete information. In assessing biosignatures, we face the problem of assigning a probability to whether an exoplanet is inhabited based on remote observations that will always be limited, especially given that *in situ* observations of even the nearest exoplanets are far in the future (e.g., Heller and Hippke 2017; Lubin 2016; Manchester and Loeb 2017). As we shall see below, Bayes' theorem quickly reveals our current ignorance about life on exoplanets. However, exposure of what we don't know points directly to what research needs to be done and which observations need to be made to increase confidence in possible detection of life on exoplanets.

Our goal is to calculate the probability that the hypothesis of life existing on an exoplanet is true given observational data that shows possible biosignatures. In terms of Bayesian statistics (e.g., see Stone (2013) for a very readable introduction), we seek the conditional probability

$P(\text{life} \mid \text{data, context})$ where “life | data, context” means “the hypothesis of life existing on an exoplanet *given* the observed data that may contain biosignatures *and* the exoplanet's context”. In this expression, “|” means “given” and the comma means “and”. The “data” are spectral and/or photometric data with possible biosignatures from an exoplanet. The “context” consists of the stellar and planetary parameters that are relevant to the possibility of life producing the spectral and/or photometric data, as illustrated in **Figure 1**.

We take the presence of life to mean the existence of a surface biosphere that is remotely detectable, which we treat as a binary variable, i.e., either an exoplanet biosphere is present or it is not. Of course, this approach cannot take into account hidden subsurface biospheres (e.g., as postulated for Europa's ocean (e.g., Chyba and Phillips 2001)) or cryptic surface biospheres that are too meager to have any effect on an exoplanet surface or atmosphere that is detectable with remote

sensing. Hidden or cryptic biospheres are not practical candidates for life detection on exoplanets, so their consideration is not relevant from our empirical perspective.

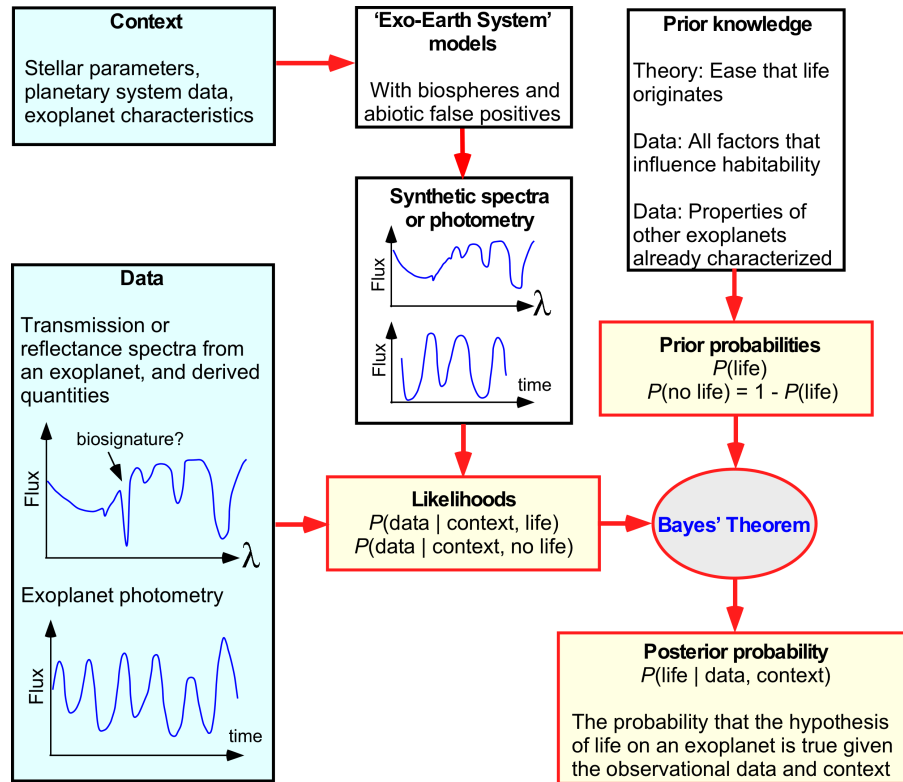


Figure 1. A Bayesian framework for biosignature assessment. Spectral and/or photometric data that may contain biosignatures are used with models to find likelihoods given the context of the exoplanet, e.g., its astrophysical environment. One likelihood is the conditional probability of those data occurring given the context and the hypothesis that the exoplanet has life. Another likelihood is the probability of the data occurring given the context and if the exoplanet has no life. These likelihoods are weighted by prior knowledge to provide a best-informed (posterior) probability that the exoplanet has life given the spectral and/or photometric data and context. *Blue* boxes signify data acquisition. *Yellow* boxes contain conditional probabilities and prior probabilities that are part of Bayes' Theorem (*gray oval*), which is expressed in eq. (1) in the main text.

With the above assumptions, the conditional probability of the hypothesis of life being present given spectral or photometric data (with possible biosignatures) and the context of the extrasolar system is:

$$P(\text{life} | \text{data}, \text{context}) = \frac{P(\text{data} | \text{context}, \text{life}) P(\text{life})}{P(\text{data} | \text{context}, \text{life}) P(\text{life}) + P(\text{data} | \text{context}, \text{no life}) P(\text{no life})} \quad (1)$$

Here, the probability $P(\text{life} | \text{data}, \text{context})$ on the left-hand side is the 'posterior probability' that we seek, which depends on a weighted assessment of the hypothesis of life's presence given the chance of the data occurring in the given context of exoplanet system properties, as expressed on the right-hand side of the equation. In the numerator and denominator, $P(\text{data} | \text{context}, \text{life})$ is the conditional probability—the 'likelihood'—of the data occurring in the given context if life is present. The likelihood of the data occurring when life is not present on the exoplanet is the probability

$P(\text{data} \mid \text{context, no life})$. Importantly, $P(\text{data} \mid \text{context, no life})$ incorporates the idea of an abiotic *false positive* detection of life. In eq. (1), we also have a ‘prior’ probability $P(\text{life})$, which is the estimated chance of life being present on an exoplanet given all current scientific knowledge at the time of an exoplanet’s assessment.

The derivation of eqn. (1) (Appendix A) assumes that parameters labeled “context” are independent of life’s presence on an exoplanet, i.e., life doesn’t influence them. This assumption is true of stellar properties, the mass and radius of the planet, the planet’s orbit, and so on. However, some environmental contextual parameters on the planet may be modulated by life, e.g., the bulk atmospheric composition and resulting climate. On Earth, the biosphere modulates all the major atmospheric gases, such as O_2 and N_2 , and most trace gases with the exception of the noble gases (e.g., Catling and Kasting 2017). Some argue that the distinction between inhabitation and habitability can become blurred (Goldblatt 2016). When contextual parameters are not independent of life, they will need to be treated as manifestations of “life”, in the “data” in the likelihoods in eq. (1) rather than as part of an independent “context”. Let us now consider the various terms in eq. (1) and what they mean for developing a practical framework of assessing biosignatures on exoplanets and assigning a probability to the presence of life.

For clarity, consider a simple example of using eq. (1). If the ‘prior’, $P(\text{life})$, is appreciable, e.g., ~ 0.5 – a fifty-fifty chance, say, that a habitable zone planet actually has life — then a possible detection of biosignatures will tend to be influenced by the estimated likelihood

$P(\text{data} \mid \text{context, life})$, i.e., the conditional probability of the occurrence of the data given the context and hypothesis of life being present. Suppose an Earth-sized exoplanet with evidence of a liquid ocean is found to have an O_2 -rich atmosphere. Under these circumstances, also suppose that the best models of the exoplanet suggest $P(\text{data} \mid \text{context, life}) = 0.80$ and $P(\text{data} \mid \text{context, no life}) = 0.25$.

Then the posterior probability of life being present on the exoplanet will be

$$P(\text{life} \mid \text{data, context}) = \frac{0.8 \times 0.5}{(0.8 \times 0.5) + (0.25 \times 0.5)} = 0.76 \equiv 76\% \quad (2)$$

Alternatively, if the prior for the presence of life is very small, i.e., $P(\text{life}) \ll 1$, then eq. (1) suggests that $P(\text{life} \mid \text{data, context})$ would tend towards $P(\text{life}) \times [P(\text{data} \mid \text{context, life}) /$

$P(\text{data} \mid \text{context, no life})]$, i.e., the value of ‘prior’ probability times the ratio of the likelihoods of the data with and without life. This posterior probability would be low and dominated by the small prior, $P(\text{life})$, unless the probability of a false positive is very small. In the former case, the “base rate” of uninhabited exoplanets, which is reflected by the small prior $P(\text{life})$, would far outweigh the number of inhabited exoplanets and false identifications of life are mathematically anticipated given that an estimated ratio $P(\text{data} \mid \text{context, life}) / P(\text{data} \mid \text{context, no life})$ may be sizeable. This Bayesian insight cautions us that exoplanet data might be over-optimistically interpreted to indicate the presence of life, if life is actually very rare in the galaxy.

In reality, of course, the probabilities in **Figure 1** will not be single numbers but functions of numerous parameters. As a result, the posterior probability that we seek, $P(\text{life} \mid \text{data, context})$, would be a more nuanced function of multi-parameter space.

The prior probability deserves discussion. One can think of $P(\text{life})$ as an estimate of the “base rate” frequency of occurrence of inhabited exoplanets, which could be restricted to exoplanets in the

habitable zone, if we are considering data from a habitable zone exoplanet. Since an exoplanet biosphere either exists or does not, the prior probability of “no life” on an exoplanet is simply

$$P(\text{no life}) = 1 - P(\text{life}) \quad (3)$$

In any future assessment of the presence of life on an exoplanet – whether designing a telescopic observatory or using telescopic data – we will always be faced with estimating a ‘prior’ probability for the presence of life, $P(\text{life})$. For example, the ubiquitous concept of the *habitable zone* is built upon the assumption that $P(\text{life})$ is spatially variable and is higher on exoplanets that orbit within a certain range of star-planet distances (Kasting 1997; Kasting *et al.* 1993; Kopparapu *et al.* 2013). Consequently, some have expressed the habitable zone as a probability density function (Zsom 2015). Physically, the habitable zone is the region around a star where an exoplanet can maintain liquid water on its surface and the conventional limits of the habitable zone are calculated with an Earth-like climate assumed to arise from a CO₂-H₂O-rich atmosphere. This assumption has been questioned because thick H₂-rich atmospheres can provide warming far beyond the conventional habitable zone, even in interstellar space (Pierrehumbert and Gaidos 2011; Seager 2013; Stevenson 1999). However, the conventional habitable zone provides a guide based on what we know about CO₂-H₂O-rich planets from a real world – the Earth – whereas habitable H₂-rich worlds remain speculative.

Essentially, $P(\text{life})$ is our best possible scientific estimate of the occurrence of life given current knowledge. Of course, this estimate would be significantly improved if we actually detect life elsewhere. Then our prior statistical information about the presence of life would expand beyond just the Earth and improve the estimate of the true frequency that life occurs.

Because extraterrestrial life has not yet been detected, the present state of scientific knowledge about the *a priori* probability of life occurring on an Earth-like exoplanet is based on two broad approaches: (1) consideration of the origin and persistence of life on a planet from laboratory and theoretical studies; and (2) the fact that detectable life exists on Earth, a planet within the Sun’s habitable zone.

Unfortunately, in the first approach, conflicting views persist about how easily life originates. Some argue that life readily emerges from a habitable environment because biochemistry naturally arises from geochemical reactions on an Earth-like planet (Smith and Morowitz 2016). Others argue that the origin of life is extremely improbable (Koonin 2012; Monod 1971). The opinions in the first approach range from $P(\text{life})$ being nearly unity on a habitable planet to being vanishingly small. However, $P(\text{life})$ is *not* a totally unknown probability where we would have to assume it is equally likely to have any value from 0 to 1. The Earth is inhabited. Consequently, $P(\text{life}) > 0$, which is an aspect of empirical astronomy to which we now turn. However, at the present stage of understanding and lack of data, the possibilities for $P(\text{life})$ range from life being very common to very rare, as has been much discussed in the literature (e.g. Carter 1983; Scharf and Cronin 2016; Spiegel and Turner 2012; Walker 2017).

There are two planets in the habitable zone of the Sun, the Earth and Mars (Kopparapu *et al.* 2013). Currently, no data from Mars conclusively shows that it ever had a biosphere (with the caveat that the situation could change if future Mars exploration uncovers evidence). In the absence of any other information, if we found an Earth-like planet in the habitable zone of a Sun-like star, a starting point—based on empirical data of the solar system—would be to assume a prior of $P(\text{life}) = 0.5$ so that $P(\text{no life}) = 0.5$ by eq. (3). One can easily criticize this approach, but with the current absence of knowledge, it is a practical point of departure, and, as we explain below, if future data from exoplanets becomes increasingly difficult to explain without invoking the presence of life, it turns out that the exact value for the assumed ‘prior’ does not matter. The path forward for assessing whether exoplanets have life is the same path that Borucki *et al.* (1996) followed in conceiving *Kepler* to

determine the number of Earth-sized planets in the Milky Way in the face of a great range of opinion on whether any stars even had such planets. Direct observation of the cosmos is the only path.

To be successful in assigning probabilities to the future detection of life on an exoplanet, astrobiology and exoplanet research must constrain the conditional probabilities $P(\text{data} \mid \text{context, life})$ and $P(\text{data} \mid \text{context, no life})$ (**Figure 1**). To constrain $P(\text{data} \mid \text{context, life})$, a framework would explore how exoplanet spectra or photometry can arise from various theoretical permutations of inhabited Earth-like planets with different biospheres (e.g., oxygenic photosynthetic, anoxygenic photosynthetic, or non-photosynthetic) under the oxidizing or reducing atmospheres that we expect are the sequence of the chemical evolution of atmospheres on rocky worlds, and will be part of the data under assessment. Similarly, to constrain $P(\text{data} \mid \text{context, no life})$, we must simulate the spectra or photometry of uninhabited planets, including planets that could plausibly produce false positives.

In order to constrain the likelihoods, we must have relevant contextual data, such as stellar parameters and physical properties of the exoplanet, as we discuss in Sec. 3.1 and 3.2. Moreover, to constrain $P(\text{data} \mid \text{context, no life})$, the contextual information needs to be used in “Exo-Earth System” models to generate synthetic exoplanet spectra or photometric data (**Figure 1**). “Exo-Earth System” models simulate many parts of an Earth-like planet, such as the interior (e.g., mantle thermal evolution), ocean, biosphere, and atmosphere. Alternatively, “Exo-Earth System” models could be used in an inverse model to fit observational data. In any case, such models are critical tools that need to be developed for a framework of assessing exoplanet biosignatures, as discussed later in Sec. 3.3.

In the future, if data from an exoplanet become more and more difficult to explain by abiotic explanations (i.e., $P(\text{data} \mid \text{context, no life})$ approaches zero), the probability of life on an exoplanet converges to 1 ($P(\text{life} \mid \text{data}) \rightarrow 1$ in eq. (1)) regardless of the choice of the ‘prior’ $P(\text{life})$ and regardless of $P(\text{data} \mid \text{context, life})$. This Bayesian insight reveals how critical it is to evaluate the plausibility of a false positive detection of life. If proposed false positive scenarios prove to be less realistic than some advocate, detecting life from Earth-like exoplanet biosignatures becomes inherently more favorable.

3. Input components in a framework of observing exoplanet biosignatures

The Bayesian framework for assessing biosignatures presented in **Figure 1** suggests some practical steps that are illustrated in a 4-component procedure for observing and interpreting biosignatures in **Figure 2**. Each component is an observational and/or analytical procedure intended to increase confidence and reduce uncertainty in a potential biosignature. For practical reasons – the schedule of new telescopic observations and when new instruments see first light – measurement components may not be sequential, as illustrated by the yellow arrows. For example, in the case of next generation telescopes, it might be the case that “internal” exoplanet properties in **Figure 1** (e.g., exoplanet mass) are determined after an exoplanet spectrum has been acquired.

In any case, the first two components are needed to gather the astrophysical and planetary “context” for a probabilistic assessment of life on an exoplanet. The first component is to characterize “external” properties of an exoplanetary system including the properties of the host star, the orbital and physical properties of the system, and the mass and radius of a target exoplanet. These properties are independent of life occurring on the planet and can be fed into Exo-Earth models to simulate exoplanet data. The second component involves characterization of the key “internal” properties of the target exoplanet, ideally including its bulk atmospheric composition, global mean climate, and surface material properties. Properties that are considered independent of life can be fed into Exo-Earth models also. Otherwise, properties would need to be considered as part of the biosignature data rather than contextual data.

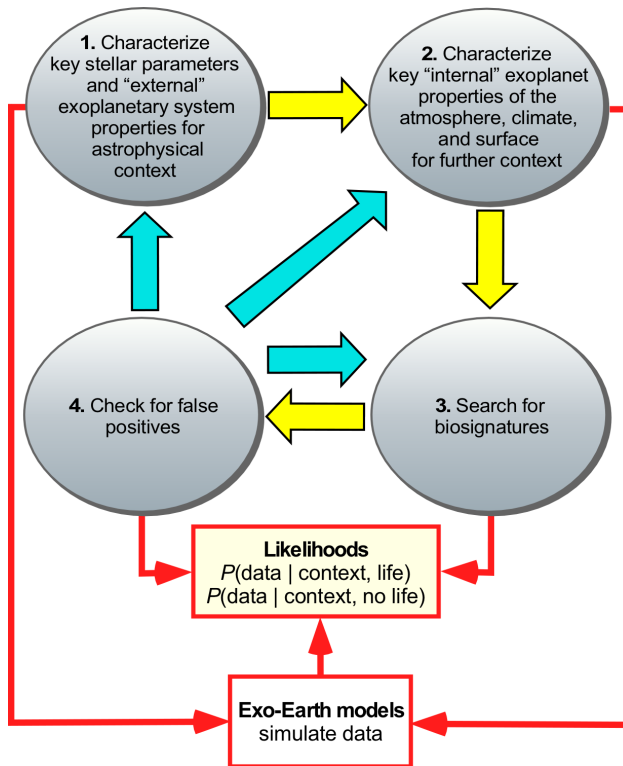


Figure 2. Four components to assess whether potential biosignatures are best explained by the presence of life. The numbered order and *yellow* arrows indicate information that an idealized observational strategy would gather sequentially, though in reality the order will likely be different. The *blue* arrows indicate how practical observation and analysis would require iteration to increase confidence in biosignature acceptance. Alternatively, following the blue arrows could aid in identification of a false positive. These components, combined with Exo-Earth models (see text), would help to constrain the likelihoods of the biosignature data occurring with and without life: $P(\text{data} | \text{context, life})$ and $P(\text{data} | \text{context, no life})$, respectively.

The third and fourth components gather and examine the spectral or photometric data that contains potential biosignatures. The third component is the explicit search for biosignatures in the reflected spectrum, transmission spectrum, or photometry of an exoplanet. These data are the ones that Exo-Earth models attempt to simulate under scenarios of life being present or absent. The fourth component is to distinguish a truly biogenic signal from all conceivable false positives. This component includes Exo-Earth modeling to test potential false positive scenarios and likely requires iteration with previous components if the possibility exists to gather more data. The result of the four components is to deduce the likelihoods given in the cream-colored box in **Figure 2**.

In the following subsections, we consider each of the 4 components of this framework in more detail. We also comment on the necessity of efforts to model an Earth-like planet and to simulate the spectral or photometric data that bear upon the possible presence of life.

3.1. Component 1: Stellar properties and “external” properties of the exoplanetary system

A potentially inhabited exoplanet is embedded within the environment of its host star, so knowledge of the properties of the host star is critical for understanding exoplanet habitability. In addition, some “external” properties of the exoplanetary system are either essential or desirable to know. **Table 1** lists potential properties of a star that it would be advantageous to determine, as well as key exoplanetary system parameters. These properties and parameters are relevant for determining whether the exoplanet is habitable or inhabited, in the following ways.

Table 1: Desirable key properties to know about the host star and exoplanetary system.

Stellar properties	Exoplanetary system properties
Age Spectral type (including effective temperature) Pan-chromatic spectrum, including the UV flux	Physical exoplanet properties - mass and radius: hence mean density and bulk composition

Activity	- presence and phase of surface
Rotation rate (related to UV emission and age)	Orbit and spin parameters:
Elemental composition	- orbit eccentricity
Whether in a multiple star system, e.g., a binary star system	- rotation rate
	- obliquity
	Other planets in the system, and their physical and orbital properties (e.g., to determine resonances)

Stellar parameters

Knowing the age of the star provides context for assessing the potential evolutionary development of an exoplanet's atmosphere and possible life. First, main sequence stars brighten with age, and this affects an exoplanet's atmosphere and habitability (Sagan and Mullen 1972; Shklovskii and Sagan 1966). As a result, the habitable zone lifetime depends on stellar evolution (Rushby *et al.* 2013). Second, a very young planetary system is probably less likely to have developed a sophisticated biosphere or the complexity of life associated with an oxygenated atmosphere because the oxygenation of the Earth's atmosphere happened about half way through Earth's history (Lyons *et al.* 2014). Some have argued, on the grounds of redox balance, that the long timescale for the Earth's atmospheric oxygenation was a result of a slow global "redox titration" of materials in the Earth's crust (Catling and Claire 2005; Catling *et al.* 2005; Zahnle and Catling 2014), which some hypotheses relate to gradual tectonic and/or mantle evolution (Holland 2009; Kasting 2013).

The spectral type and effective temperature of a star are essential parameters for estimating the incident flux on the exoplanet, which is a key parameter for the planetary energy budget, climate, and possible habitability (e.g., Catling and Kasting 2017; Kopparapu *et al.* 2013; Pierrehumbert 2010). Issues of climate are discussed further below in Sec. 3.2.

The pan-chromatic spectrum, including the UV flux, provides an essential input for models of the atmospheric chemistry, climate, and atmospheric escape of exoplanets (Linsky and Güdel 2015). The UV must be short enough to include the Lyman-alpha wavelength of 121 nm, which causes much of the photolysis of molecules such as CH₄. The spectral energy distribution (SED) is needed to understand atmospheric chemistry because it affects the reactions of key molecules of interest on a habitable exoplanet, such as CO₂, CH₄, O₂ and H₂O (Segura *et al.* 2003). In particular, the abundances of potential biosignature molecules such as CH₄ in oxic atmospheres are strongly affected by the magnitude of the near-UV flux below 310 nm because this wavelength region is important in generating the OH (hydroxyl) radical, which is a key oxidizing species (Segura *et al.* 2005). Indeed, the most common stars, M-dwarfs, have a lower flux in the near-UV compared to the Sun, so that for the same biogenic CH₄ flux as the Earth, the CH₄ abundance attains a much higher and more detectable level depending upon the exact SED (Rugheimer *et al.* 2015; Segura *et al.* 2005). The SED is also necessary to run photochemical models that disentangle possible gaseous biosignatures from abiotic false positives, as explored for O₂ and O₃ (Domagal-Goldman *et al.* 2014; Gao *et al.* 2015; Harman *et al.* 2015; Meadows 2017; Tian *et al.* 2014).

The SED also directly affects the habitable zone. Near the inner edge of the habitable zone, a planet orbiting a cooler star has a lower albedo in the near-infrared and reaches the "moist greenhouse" limit of significant water loss at a lower incident flux than a warmer star due to near-

infrared absorption by H₂O and CO₂ and weaker Rayleigh scattering (e.g., Catling and Kasting 2017 p.427-430; Kopparapu *et al.* 2013). Near the outer edge of the habitable zone, the ice-albedo feedback is weaker for a cooler star because sea ice and snow are less reflective in the near-infrared (Joshi and Haberle 2012; Shields *et al.* 2013).

Stellar activity is dominated by the stellar magnetic field evolution, which affects flare occurrence, the intensity of a stellar wind, and the emission at UV and X-ray wavelengths. For habitable zone planets around M stars, intense stellar winds may compress planetary magnetospheres, enough to make a planetary surface susceptible to cosmic ray exposure (Griessmeier *et al.* 2005). Consequently, knowledge of the stellar activity is desirable. It has also been proposed that magnetospheric compression due to strong coronal mass ejections from young stars allow energetic particles to enter the atmosphere and induce upper atmospheric chemistry. The resulting reactions may fix nitrogen and produce gases such as N₂O (Airapetian *et al.* 2016). Modeled upper atmosphere N₂O at part per million levels could present a false positive for N₂O, which is a biogenic gas on Earth. In contrast, modeled ground-level concentrations of N₂O are \ll 1 ppbv and so would produce negligible greenhouse warming with little impact on habitability given that Earth's modern concentration of N₂O of \sim 0.32 ppmv produces $<$ 1 K of warming (Schmidt *et al.* 2010).

Stellar activity is related to the rotation rate of a star (Pallavicini *et al.* 1981; Ribas *et al.* 2005), so knowledge of the stellar rotation rate would help characterize the shortwave emission of a host star, particularly the large Lyman-alpha output at 121 nm (Linsky *et al.* 2013), which produces photons that drive photolysis reactions in planetary atmospheres. Stellar rotation can be measured in various ways (Rozelot and Neiner 2009; Slettebak 1985): photometric tracking of features on the star (such as starspots), Doppler shift in the stellar spectrum, using a star's oblateness (van Belle 2012), or using the Rossiter effect that distorts the radial velocity curve in rotating binary star systems.

The elemental composition of the parent star, while not essential for biosignature interpretation *per se*, is desirable to help understand the potential bulk composition of the nebula that gave rise to the exoplanet. Potentially, we could gain insight into the bulk composition of the exoplanet. Elemental composition gives metallicity—the proportion of elements other than hydrogen or helium expressed on a log₁₀ scale relative to the Sun—is a parameter commonly used in astronomy (where solar is 0, metal poor $<$ 0, and metal-rich $>$ 0). A correlation between gas giant planet occurrence and stellar metallicity exists (Fischer and Valenti 2005; Johnson *et al.* 2010) and metallicity differences also appear to be linked to the occurrence of rocky planets and small gas-rich planets (Wang and Fischer 2015). At present, apart from the bulk density, the only insight into the bulk composition of an exoplanet comes from indirect inference from the host star's elemental composition through the spectrum of its photosphere (Gaidos 2015). An exoplanet's bulk composition is potentially important for the planet's possible geological evolution.

Finally, about a third of stars in the Milky Way are in binary or multiple systems (Lada 2006), and the long-term habitability of exoplanets may be affected by the presence of a nearby star (David *et al.* 2003). A key concern is whether habitable zone planets in multiple star systems have stable orbits on sufficiently long timescales to be compatible with an origin and evolution of life (perhaps \sim Gyr). Additionally, multi-star systems can host the remnants of an evolved star (e.g., a white dwarf), which would indicate that the system, at some point, endured dramatic changes during the post-main sequence evolution of the evolved companion. Consequently, it would be desirable to know if the exoplanet host star is part of a multiple star system to understand whether the exoplanet may have

been subject to a history that makes it a less viable candidate for inhabitation. Also, sometimes the age of a star is determined from the better known age of a companion, e.g., Proxima Centauri's ~ 4.8 Ga age is estimated from that of Alpha-Centauri (Bazot *et al.* 2016).

Planetary system parameters

Among basic physical properties, the exoplanet mass and radius provide the mean density of the exoplanet and the gravitational acceleration at the surface, g . The mean density sets overall constraints on rockiness and the possibilities for the size of an iron-rich core. Consequently, an Earth-like mean density would lend confidence that an exoplanet is truly rocky and not a migrated icy body or a planet with a large gas envelope. An accurate internal structure model of an exoplanet, of course, remains undefined without a moment of inertia. Some proposals have been made for determining the moment of inertia of exoplanets from the influence of a gravitational quadrupole field and tidal dissipation characteristics in the case of certain orbital architectures of exoplanetary systems (Batygin *et al.* 2009; Batygin and Laughlin 2011; Becker and Batygin 2013; Mardling 2010).

The gravitational acceleration, g , of an exoplanet is necessary for understanding a variety of basic physical parameters of the atmosphere, including the scale height and lapse rate (see Sec. 3.3.2). These parameters are needed to accurately estimate the abundances of gases in an exoplanet's atmosphere from retrievals and a possible inference of the surface temperature of the planet from calculated greenhouse warming if surface temperature is not directly observable from thermal emission.

The value of g also affects spectral interpretations. For example, Rayleigh scattering depends on column number density, which depends on g . Transit spectra are sensitive to the pressure scale height of an atmosphere, which is an inverse function of g .

Knowledge of the rotation rate of an exoplanet is highly desirable for a basic model of the climate, and hence habitability. The rotation rate controls both the temporal distribution of irradiation from the host star and the dynamical regime of an exoplanet's atmosphere (Showman *et al.* 2013). Essentially, slowly rotating planets tend to be in "all tropics" dynamical regimes with equatorial superrotation. Fast rotation causes structure in the climate system with latitude: smaller and weaker Hadley cells, smaller eddy length scales, and more jets (Kaspi and Showman 2015). If the rotation period becomes comparable to or greater than the radiative relaxation time, strong day-night contrasts emerge, generating thick dayside clouds that might extend habitability closer to the host star than the traditional inner edge of the habitable zone (Kopparapu *et al.* 2016; Way *et al.* 2016; Yang *et al.* 2014). In principle, the rotation rate can be inferred several ways: (1) from brightness or color variations as a planet rotates (including the effect of continental or persistent cloud patterns) (Cowan *et al.* 2009; Ford *et al.* 2001; Livengood *et al.* 2011; Oakley and Cash 2009; Palle *et al.* 2008); (2) from the Doppler shift of absorption features during ingress and egress of a transiting exoplanet (Spiegel *et al.* 2007); or (3) from comparing thermal phase curve with rotation-dependent models (Rauscher and Kempton 2014).

Knowledge of an exoplanet's obliquity (axial tilt) would give a more complete picture of habitability through the effect of seasonality on heat transport around the planet. A large obliquity may potentially allow for large temperature excursions on a planet's surface, which would affect habitability (Williams *et al.* 1996). Alternatively, obliquity with high frequency variations could suppress ice-albedo feedback and enlarge the habitable zone outwards (Armstrong *et al.* 2014).

However, determining exoplanet obliquity would require analyses of temporal color changes at different orbital phase angles (Kawahara 2016; Kawahara and Fujii 2010).

The orbital eccentricity is also essential for a model of the possible atmospheric evolutionary history, the seasonal climatic variations on an exoplanet, and potential planet-planet dynamical interactions. While climate variations alone due to extreme eccentricity may not compromise habitability (Williams and Pollard 2002), planets with very high eccentricity could experience large tidal heating that could desiccate a planet through water loss (Barnes *et al.* 2013). On the other hand, tidal heating could also prevent global snowball states (Barnes *et al.* 2008; Reynolds *et al.* 1987).

Knowing about other planets and their properties in an extrasolar system could be important for deducing the formation history of the star-planet system and possible evolutionary path of the exoplanet of interest. For example, other planets might be in mean orbital motion resonances with habitable zone planets, as in the system of 7 planets around the star TRAPPIST-1 (Gillon *et al.* 2017). Such resonances can cause tidal heating and be related to a history of planet migration, which affects whether planets have moved into or out of a habitable zone over time.

3.2. Component 2: The “internal” properties of the exoplanet atmosphere, climate and surface

A planet inside a habitable zone is not necessarily habitable. Stellar and exoplanetary system external properties provide context for understanding an exoplanet’s habitability, but direct measurements concerning an exoplanet’s “internal” properties are also needed to assess habitability, including bulk atmospheric composition and structure, climate, and surface state (**Table 2**).

Measurements such as the surface temperature or the detection of liquid water on the surface would provide direct confirmation that an exoplanet is habitable (Robinson 2017), following the conventional definition of a habitable planet as one with a solid surface that has an extensive covering of liquid water (Kasting *et al.* 1993). Other data in **Table 2** would increase confidence that the exoplanet is Earth-like in detail rather than just similar in size and mass, like Venus.

Table 2: Desirable “internal” general properties of an atmosphere and surface to know about a potentially habitable exoplanet.

Climatic and surface properties	Atmospheric properties
Average surface emission temperature, T_{surfe}	Bulk composition and redox state
Bond albedo, A_B	Surface barometric pressure
Effective temperature, T_{eff}	Clouds or haze composition and structure
Surface phase:	Vertical structure
- liquid water or ice	Mixing ratios of key trace species:
- silicates	- H ₂ O from evaporation
	- SO ₂ or H ₂ S from volcanism
	- Greenhouse gases (see Table 3)

Climatic and surface parameters and properties

Knowing if the global average surface emission temperature T_{surfe} of an exoplanet is compatible with liquid water is a highly desirable piece of information and possibly essential to provide high confidence of the detection of life on an exoplanet from biosignatures (Sec. 3.3). On a planet with a thick atmosphere and surface water, the value of T_{surfe} must also be below some upper limit for the stability of biomolecules. On Earth, deep-sea hyperthermophilic microbes can grow at

121°C and survive up to 130°C (Kashefi and Lovley 2003). But many biomolecules rapidly degrade above 150°C (Somero 1995; White 1984) even with the stabilizing influence of high pressure (Lang 1986). Thus, a conservative upper limit on T_{surfe} for a habitable planet is $T_{\text{surfe}} < 425$ K. A surface temperature exceeding 647 K – water’s critical temperature at which water can only exist as vapor – is the likely firm physical limit for habitability.

In principle, T_{surfe} could be inferred directly if an exoplanet is observed over a wavelength region in which its surface emits thermal radiation to space through a nearly transparent window where the atmosphere does not absorb. For example, the Earth’s surface temperature can be observed from space through an atmospheric window at wavelengths between 8 and 12 μm . However, thick hazes, clouds, or a highly absorptive and scattering atmosphere can prohibit a direct view of a planet’s surface across a very broad range of wavelengths. In the solar system, Venus’ surface is obscured because visible and infrared radiation is scattered or absorbed and emitted from far above the surface (Titov *et al.* 2013). Multiple cloud layers of sulfuric acid droplets scatter light, while collision-induced absorption and far-wing pressure broadening of CO_2 at lower altitudes accounts for significant infrared (IR) opacity.

Two key parameters that govern a rocky exoplanet’s average climate are the total stellar irradiance S_* (in W m^{-2}) at the exoplanet’s orbital position—considered in the previous section, 3.3.1, as an “external” property—and the exoplanet’s Bond albedo, A_B , considered here as an “internal” property intrinsic to the exoplanet (**Table 2**). These two parameters determine the planet’s effective radiating temperature T_{eff} . Then, T_{eff} , with the planet’s greenhouse effect, determines the average surface emission temperature T_{surfe} . These quantities are related as follows (see, e.g., Catling and Kasting (2017), p.34-36):

$$T_{\text{surfe}} = T_{\text{eff}} + \Delta T_{\text{greenhouse}} = \left[(1 - A_B) \frac{S_*}{4\sigma} \right]^{1/4} + \Delta T_{\text{greenhouse}} \quad (4)$$

Here, σ is the Stefan-Boltzmann constant ($5.67 \times 10^{-8} \text{ W m}^{-2} \text{ K}^{-4}$) and $\Delta T_{\text{greenhouse}}$ is the temperature increase of the average surface emission temperature due to the greenhouse effect of the exoplanet’s atmosphere.

Clearly, the exoplanet effective blackbody temperature T_{eff} can be calculated if the Bond albedo and incoming stellar flux are known. On the Earth, values of parameters in eq. (4) are $S_* = 1361 \text{ W m}^{-2}$ (Kopp and Lean 2011), $A_B = 0.3$ (Palle *et al.* 2003; Stephens *et al.* 2015), $T_{\text{eff}} = 255$ K, $T_{\text{surfe}} = 288$ K, and $\Delta T_{\text{greenhouse}} = 33$ K (Schmidt *et al.* 2010). Although exoplanet surveys frequently assume a default Bond albedo around 0.3 to estimate the effective temperature of a rocky planet (e.g., Sinukoff *et al.* 2016), in fact, planets with atmospheres in our solar system have a wide range of Bond albedos from 0.76 on Venus (Moroz *et al.* 1985) to 0.25 on Mars (Pleskot and Miner 1981). Moreover, the extremes of Bond albedo in the solar system are comets at ~ 0.04 and Enceladus at 0.89 (Encrenaz 2014; Howett *et al.* 2010). Bond albedo is a more important parameter for Earth-like exoplanets than for giant planets because surface temperature is a key to habitability.

The single most important surface feature that could be observed to enhance our confidence in the habitability and possible inhabitation of an exoplanet would be liquid water. In principle, detection of a glint spot of specular reflection indicates the presence of a large body of liquid water (Robinson *et al.* 2010; Sagan *et al.* 1993; Williams and Gaidos 2008). Glint could be observed as an increasing reflectivity in an exoplanet’s crescent phase (Palle *et al.* 2003; Qiu *et al.* 2003). However, glint alone just indicates a liquid, rather than water per se. For example, hydrocarbon lakes on Titan produce glint (Soderblom *et al.* 2012; Stephan *et al.* 2010). So the environmental context of the surface temperature remains crucial even if glint is detected.

A second way to infer an ocean is through the detection of polarized reflected light. Unpolarized light incident on an ocean surface will be reflected with some degree of polarization, which peaks at the Brewster angle. This angle depends on the change in refractive index between the atmosphere and ocean, and, e.g., is 53° for an air-water interface. Consequently, the fraction of the light that is polarized could be used to infer if an exoplanet has an ocean (Stam 2008; Williams and Gaidos 2008; Zuger *et al.* 2010).

Finally, a third proposed way to infer an ocean is from a very attenuated light curve of thermal emission from an Earth-like planet with seasonality, which may indicate a high thermal inertia that would require an ocean (Gaidos and Williams 2004).

An additional desirable surface feature of an exoplanet to determine would be spectral evidence of a silicate surface indicating a rocky planet. The presence of Si-O on airless rocky exoplanets would produce features in thermal infrared emission bands (Hu *et al.* 2012), but these would be obscured by thermal infrared emission in a thick atmosphere at temperatures typical of habitability. However, high-resolution reflectance spectroscopy might be able to distinguish broad iron-related absorption bands from narrower atmospheric molecular features.

“Carbon planets”, which are predicted to form in a C-rich and O-poor protoplanetary disks, would also have solid surfaces but would be water-poor and uninhabitable to life as we know it (Bond *et al.* 2010; Carter-Bond *et al.* 2012; Elser *et al.* 2012; Moriarty *et al.* 2014). Planet formation models suggest that high C/O ratio disks could produce planets with iron cores, mantles of SiC or TiC, and diamond or graphite crusts. If such planets exist, reactions with carbon of any water delivered to the planet during accretion could preclude the presence of liquid water, although liquid hydrocarbons on the surface might be possible.

Atmospheric parameters and properties

An estimate of an exoplanet’s bulk atmospheric composition is highly desirable because it affects all aspects of the atmosphere’s behavior: radiation, convection and dynamics. The bulk atmospheric composition must be known to apply an equation of state to an exoplanet atmosphere. If we use the ideal gas law, $P = \rho \bar{R}T$ (for pressure P , temperature T , and air density ρ), the specific gas constant \bar{R} is set by bulk atmospheric composition using $\bar{R} = R / \bar{M} = k / \bar{m}$, where \bar{M} is the mean molar mass (in kg mol^{-1}), \bar{m} is the mean molecular mass ($\bar{M} = N_A \bar{m}$ where N_A is Avogadro’s number), and k and R are Boltzmann’s constant and the molar ideal gas constant, respectively. Along with gravity, the bulk composition also determines the atmospheric scale height, $H = \bar{R}\bar{T} / g$ for a mean temperature \bar{T} . Furthermore, bulk composition fixes the specific heat capacity at constant pressure c_p , which sets the dry adiabatic lapse rate Γ_{ad} (decline of temperature with altitude in the convective part of a dry troposphere), given by $\Gamma_{\text{ad}} = g/c_p$.

Molar mass and heat capacity affect the dynamics of an atmosphere, and thus the climate and associated observables. On a tidally-locked body, atmospheres with bigger molar mass tend to have larger day-night temperature differences, narrower super-rotating jets, and smaller zonal wind speeds with more latitudinal variation (Zhang and Showman 2017). Hence, the bulk atmospheric composition could affect thermal phase curves.

Atmospheres on Earth-like habitable planets are expected to contain CO_2 , which is an important gas for a number of reasons. On Earth, environmental feedbacks on CO_2 levels maintain

long-term habitability over ~ 1 m.y. timescales through the carbonate-silicate geochemical cycle (Kasting and Catling 2003; Krissansen-Totton and Catling 2017; Walker *et al.* 1981). But CO_2 is also valuable for another reason: it should be a well-mixed atmospheric constituent that allows retrieval of atmospheric temperature structure from spectral data, which is necessary to retrieve the abundances of other gases, including possible biosignature gases (see below). In addition, on a habitable world, the presence of CO_2 provides a possible substrate for biological carbon fixation (e.g., Raven *et al.* 2012).

Other possible bulk gases, such as N_2 are more challenging to detect. For N_2 partial pressures above 0.5 bar, collisional pairs of nitrogen, i.e., $\text{N}_2\text{-N}_2$, produce a detectable absorption signal in transit transmission or reflectance spectra at 4.15 μm in the wings of the strong 4.3 μm CO_2 absorption band (Schwieterman *et al.* 2015b) (see **Table 3**).

It is also worth considering the possibility of detecting bulk anti-biosignature gases that may be abundant in some types of atmosphere. An *anti-biosignature* is any substance, group of substances, or phenomenon that provides evidence against the presence of life. One anti-biosignature candidate is carbon monoxide, CO (Gao *et al.* 2015; Zahnle *et al.* 2008), which has absorptions at 4.67 (strong), 2.34 (weak) and 1.58 μm (very weak) (Wang *et al.* 2016). On Earth, CO is a gas that is readily consumed by microbes in the presence of water, serving both as a metabolic substrate and carbon source (Ragsdale 2004). So biology should remove CO and suppress its abundance. The presence of abundant CO would also tend to argue against a liquid water surface because the photochemical sink of CO is the OH radical, which atmospheric chemistry should produce in relative abundance from near-UV photolysis if water vapor evaporates from an ocean. Another potential anti-biosignature is the co-existence of abundant H_2 and CO_2 . These gases are a redox couple for microbial CH_4 production, which molecular phylogenetic studies suggest may be one of the most primitive metabolisms on Earth (Weiss *et al.* 2016). The primitive nature of this metabolism suggests that it may be easy to evolve.

Even if atmospheric bulk composition is incompletely known, it might be possible to infer the redox state of an atmosphere. Redox information is desirable because it can indicate the evolutionary stage of an Earth-like atmosphere, as well as Mars- Titan- or Venus-like states, and also the most plausible chemical composition of aerosols. The redox state of the atmosphere can also impact the ocean chemistry, climate, and degree to which different metabolisms are beneficial to biology.

‘Reducing’ or ‘oxidizing’ are two fundamental chemical categories of atmospheres, and knowing whether an exoplanet atmosphere is one category or the other constrains the overall atmospheric chemistry. Reducing atmospheres are relatively rich in reducing gases, such as the hydrogen-bearing gases H_2 , CH_4 , C_2H_6 , and NH_3 , and also potentially CO, whereas oxidizing atmospheres generally contain CO_2 , possibly O_2 , and only trace levels of reducing gases. Reducing atmospheres at low or moderate temperatures tend to contain organic hazes, as observed on Titan and the giant planets of the solar system. Oxidizing atmospheres can contain widespread H_2SO_4 aerosols but not Titan-like global organic hazes. The Earth began with a chemically reducing atmosphere that became increasingly oxidized over its history (reviewed by Catling and Kasting (2017)). Looking for the spectral signature of reducing gases, as listed in Table 3, is therefore important. Even if the bulk composition cannot be fully determined, it might be possible to infer the redox state from the relative prevalence of oxidized or reduced gases.

Surface barometric pressure is an indicator of habitability (as sufficient pressure is required to prevent the rapid sublimation of any surface liquid water), and, when combined with a measure of g , surface pressure enables the inference of the total atmospheric mass. As with any spectrally inferred surface property, surface pressure can only be measured (or inferred) if the continuum level in a spectrum probes the deepest atmospheric levels. In general, the width of pressure-broadened molecular absorption bands can help to constrain atmospheric pressure. For reflected-light observations, Rayleigh scattering can indicate pressure, as can the detection of Raman scattering at UV wavelengths (Oklopčić *et al.* 2016). Also, collision-induced absorption features, where the opacity depends on the number densities of the colliding molecules, have been proposed as barometers due to their strong dependence on pressure (Misra *et al.* 2014). Finally, for the specific case of tidally-locked rocky exoplanets, the day-night temperature gradient is controlled by surface pressure, equilibrium temperature, and composition (through specific gas constant \bar{R} and heat capacity), so that, in principle, thermal phase curves that determine day-night temperature contrasts might be used for inferring surface pressure (Koll and Abbot 2016).

Clouds and hazes are observed on all planets in the solar system with thick atmospheres, although some planets, such as Earth, are much less cloudy than others, such as the giant planets. Clouds occur when a condensable constituent super-saturates and forms particles (e.g., water vapor turning to liquid droplets when uplifted to a colder altitude), whereas hazes are condensable species produced by photochemical reactions (e.g., organic smog on Titan) (Marley *et al.* 2013). The presence of cloud would indicate the presence of a volatile phase, which could be water if spectra are consistent with liquid water drops or water ice particles. Clouds also provide information on the temperature-pressure profile of the planet, as they indicate a liquid or solid phase of a species in the equilibrium state at a layer in the atmosphere. This information can be valuable if the altitude (or pressure level) of the clouds can be determined. A possible sign of clouds, albeit non-unique, is albedo. Cloudy planets, like those in the Solar System, tend to have relatively high geometric albedos (Demory *et al.* 2013; Marley *et al.* 2013). Brightness variability at timescales distinct from the rotational timescale could also indicate clouds, whose distributions change due to weather or climate.

The presence of clouds or hazes has consequences for detecting biosignatures. Clouds and hazes tend to diminish the sensitivity of transit spectra to the deep atmosphere (Knutson *et al.* 2014; Kreidberg *et al.* 2014; Robinson 2017; Robinson *et al.* 2014). Also, substantial cloud cover can mute absorption features in reflectance spectra (Kaltenegger *et al.* 2007; Rugheimer *et al.* 2013).

Hazes could be the photochemical products of volcanic gases or biogenic gases, which in certain chemical cases could indicate a volcanically active body (Kaltenegger *et al.* 2010; Misra *et al.* 2015) or a potentially inhabited early-Earth-like body (Arney *et al.* 2016), respectively. A $1/\lambda^4$ slope (where λ is wavelength) of the continuum in the UV-visible part of the spectrum could indicate Rayleigh scattering of particular molecular or aerosol species and possible transparency of an atmosphere (i.e., high single scattering albedo) caused by the haze-free chemistry of an oxidizing atmosphere. For example, such scattering by gases in a relatively haze-free atmosphere causes the Earth to appear remotely from a great distance as a “Pale Blue Dot” (Krissansen-Totton *et al.* 2016b; Sagan 1994). Conversely, transmission and scattering characteristics can also indicate the presence of hazes. In transit transmission spectroscopy, a long pathlength means that a haze with only modest vertical optical depth can cause substantial broadband opacity (Fortney 2005). Thus, the spectrum

produced by the scattering of a haze is very different to a purely gaseous medium (Knutson *et al.* 2014; Kreidberg *et al.* 2014; Robinson *et al.* 2014).

The structure of an atmosphere is scientific shorthand for the vertical temperature structure (because pressure and density are then defined by hydrostatics and an equation of state), and the better the thermal structure is known, the better one can retrieve gas abundances from thermal infrared spectral data. The structure of strong absorption bands of a well-mixed gas is required to retrieve atmospheric structure. In the near infrared, CO₂ has a fundamental absorption at 4.3 μm, strong absorptions at 2.7 and 2.0 μm, and weaker absorptions at 5.2, 4.8, 1.6 and 1.4 μm (**Table 3**). Weak bands can also be used for other information. In early remote sensing of the solar system, the CO₂ content found from the weak 1.6 μm band of CO₂ was used to estimate the surface pressure on Mars (Owen and Kuiper 1964). With sufficient spectral resolution, strong CO₂ absorption bands can be inverted to retrieve the vertical temperature profile above the surface of a planet or above a cloud surface (e.g., Rodgers 2000; Twomey 1996). Once a thermal profile is calculated, one can retrieve the abundances of minor species that could provide information about the environment (the presence of abundant H₂O) or potential biosignatures (e.g., O₃ or CH₄) (e.g., Drossart *et al.* 1993).

Key trace species in the atmosphere could provide important insights into habitability. Earth's reflectance spectrum contains a large number of water vapor absorption features. We should expect a habitable exoplanet with surficial liquid water to have substantial gas-phase H₂O in its atmosphere as a result of evaporation and so a large number of H₂O vapor absorption bands should be present. In the near-IR, key H₂O absorption bands are centered at 2.7, 1.87, 1.38, 1.1, 0.94, 0.82, and 0.72 μm. Analysis of water vapor's vibration-rotation bands could be used to infer a large H₂O vapor abundance in the atmosphere. If the planet's surface temperature is suitable, a large amount of water vapor could only be explained by evaporation from a large body of liquid water on a planet's surface rather than the cool top of a steam atmosphere.

Liquid or frozen water on a surface has spectral features that are broadened and shifted to different wavelengths compared to water vapor. Stretching vibrations are shifted to longer wavelengths in the condensed phase: from 2.66 and 2.73 μm in water vapor to 2.87 and 3.05 μm in liquid, to 3.08 and 3.18 μm in ice (Fletcher 1970, his Table 2.1). Formation of a hydrogen bond weakens the 'spring constant' for the covalent bond. But the hydrogen bonding constrains bending, so the bending 'spring constant' becomes stiffer and bending vibrations are shifted to shorter wavelength: from 6.27 μm in vapor to 6.10 μm in ice (Warren and Brandt 2008). Condensed phases also have much smoother absorption spectra compared to the jagged line spectra of gases (e.g., see Wozniak and Dera 2007 p.54). Loosely, one can think of this as extreme collision broadening, since in a condensed phase the molecules are in contact, so always "colliding".

Other trace gases could potentially indicate volcanism, such as SO₂, H₂S and HCl (Kaltenegger *et al.* 2010). The lack of SO₂ and HCl spectral absorption has been used as evidence for absence of volcanic activity on Mars, for example (Hartogh *et al.* 2010; Krasnopolsky 2012). Conversely, these gases could be used to look for active volcanism. In both oxic and weakly reducing atmospheres, some SO₂ and H₂S can be oxidized to sulfate aerosols. Consequently, transient increases in near-IR extinction in transmission spectroscopy due to aerosol loading could be a signature of pulses of explosive volcanism on an exoplanet (Misra *et al.* 2015). H₂SO₄ itself also has absorption features in the thermal IR and near-IR (Palmer and Williams 1975; Pollack *et al.* 1978).

Table 3: Specific atmospheric substances, their spectral bands in the UV-visible to thermal-IR, and their significance for providing environment context for establishing whether an Earth-like exoplanet is truly habitable. Also noted is the interpretation of potential biosignature gases.

Substance	Spectral band center or feature, μm	Significance for the planetary environment and habitability
CO ₂	15, 4.3, 4.8, 2.7, 2.0, 1.6, 1.4, 0.1474, 0.1332, 0.119	<ul style="list-style-type: none"> - Non-condensable greenhouse gas at $T > 140$ K (i.e., except at the outer edge of a conventional habitable zone) - Well-mixed gas, enabling retrievals of atmospheric structure - Could be an <i>anti-biosignature</i> if it coexists with a large amount of H₂ - Could be a substrate for biological C fixation
N ₂	0.1-0.15 For N ₂ -N ₂ : 4.3, 2.15	<ul style="list-style-type: none"> - Pressure-broadening that enhances the greenhouse effect
O ₂	6.4, 1.57, 1.27, 0.765, 0.690, 0.630, 0.175-0.19 For O ₂ -O ₂ : 1.27, 1.06, 0.57, 0.53, 0.477, 0.446	<ul style="list-style-type: none"> - Possible bulk constituent that enhances greenhouse effect through pressure broadening and weak thermal IR absorption (Also a possible biosignature and hence also in Table 4).
O ₃	>15 (rotation), 14.5, 9.6, 8.9, 7.1, 5.8, 4.7, 3.3, 0.45-0.85, 0.30-0.36, 0.2-0.3	<ul style="list-style-type: none"> - Possible indicator of O₂ from which it derives - Greenhouse gas
H ₂ O	continuum, > 20 (pure rotation), 6.2, 2.7, 1.87, 1.38, 1.1, 0.94, 0.82, 0.72, 0.65, 0.57, 0.51, 0.17, 0.12	<ul style="list-style-type: none"> - Condensable greenhouse gas - Abundances near saturation inferred from spectral features may suggest a wet planetary surface or clouds
CO	4.67, 2.34, 1.58, 0.128-0.16	<ul style="list-style-type: none"> - <i>Anti-biosignature</i> gas - May indicate lack of liquid water
H ₂	2.12, near-IR continuum, <0.08 continuum	<ul style="list-style-type: none"> - <i>Anti-biosignature</i> gas if a relatively high abundance co-exists with abundant CO₂ - Pressure-broadening that enhances the greenhouse effect - Greenhouse effect from pressure-induced absorption with self and other key species (e.g., CO₂, CH₄)
CH ₄	7.7, 6.5, 3.3, 2.20, 1.66, <0.145 continuum	<ul style="list-style-type: none"> - Greenhouse gas - In the absence of oxidized species, could indicate a reducing atmosphere. Also a potential biosignature (Table 4)
C ₂ H ₆	12.1, 3.4, 3.37, 3.39, 3.45, <0.16 continuum	<ul style="list-style-type: none"> - Together with CH₄, in the absence of oxidized species, could indicate a reducing atmosphere
HCN	14.0, 3.0, <0.18 continuum	<ul style="list-style-type: none"> - In the absence of oxidized species, could indicate a reducing atmosphere
H ₂ S	7, 3.8, 2.5, 0.2	<ul style="list-style-type: none"> - Potentially volcanic gas
SO ₂	20, 8.8, 7.4, 4, 0.22-0.34	<ul style="list-style-type: none"> - Potentially volcanic gas
H ₂ SO ₄ (aerosol)	11.1, 9.4, 8.4, 3.2*	<ul style="list-style-type: none"> - Transient behavior potentially indicates active volcanism - May indicate an oxidizing atmosphere - Climate effects (cloud condensation nuclei; albedo)
Organic haze	continuum opacity in vis-NIR	<ul style="list-style-type: none"> - Indicates a reducing atmosphere with CO₂/CH₄ < 0.1 - May derive from biogenic or abiotic methane - Climate effects (anti-greenhouse effect; shortwave absorption)
Rayleigh scattering	0.2-1	<ul style="list-style-type: none"> - May indicate cloud-free atmosphere and help constrain the main scattering molecule (bulk atmospheric composition)
Clouds	UV, vis, NIR, TIR	<ul style="list-style-type: none"> - Climate effects - Radiative transfer calculations with scattering (Rayleigh and Mie multiple

*Exact wavelengths depend on the concentration of H₂SO₄ and size distribution of the aerosols

3.3. Component 3: Potential biosignatures in the spectral data

Future telescope projects and missions plan to search for potential biosignatures in the data from habitable worlds, which is the third component of our framework. Assessing whether the planet is truly habitable with liquid water on the surface is part of the “internal” climatic, atmospheric and surface properties of an exoplanet (Component 2 in **Figure 2**). For Component 3, we are focused on biogenic matter that has distinct signatures in remote sensing data. Candidate biogenic constituents include gases, aerosols, or surface pigments. The field of remotely detectable biosignatures is still in its infancy, however, and proposals for alternative biosignatures and classes of biosignature are described in Walker et al., *this issue*. Here, we focus on commonly accepted biosignatures and specific examples. Component 3 in our framework identifies the spectral signatures of a variety of biogenic molecules, and then determines whether their biological nature is corroborated by the environmental context or the presence of additional biosignatures.

Candidate biogenic gases and their concentrations or column abundance.

Based on the detectability of Earth-based life, it is expected that the most detectable biogenic substances in exoplanetary spectra will be gases. For practical purposes, a *biosignature gas* is one that accumulates in a planet’s atmosphere to a detectable level (e.g., Seager and Bains 2015). Although biology produces a wide variety of gases, if there is no physical scenario where a certain gas could reach high enough concentrations in an exoplanet atmosphere to be detectable then it is not an effective biosignature. For example, around a Sun-like star, photochemical destruction prevents the build up of remotely detectable levels of many organic sulfur gases for biospheric fluxes into the atmosphere that are comparable to those of the modern Earth (Domagal-Goldman *et al.* 2011). Similarly, ammonia has difficulty accumulating to detectable concentrations on planets with Earth-like amounts of radiation from their host stars, even in relatively reduced atmospheres (Sagan and Chyba 1997). Because the abundance of a gas depends both on sink and source fluxes, we have to account for the magnitude of both plausible sinks and biological sources.

A variety of proposed spectral gaseous biosignatures are shown in **Table 4**. Some these gases also have atmospheric or climatic significance and so were previously listed in **Table 3**. The biogenic nature of each species is informed by our knowledge of terrestrial biology. However, in general, a redox reaction as a source of metabolic energy is a universal aspect of chemistry that should apply to life anywhere. Consequently, photosynthetic O₂ (from splitting water using sunlight) or N₂O (from reducing oxides of nitrogen with organic carbon) are ways that microbe-like entities anywhere could gain energy chemically for conducting carbon fixation or other biological processes. Walker et al., *this issue*, expand further on universal aspects of life.

Most currently accepted biosignatures consist of spectral evidence of a biogenic gas molecule. The only accepted surface pigment biosignature is the “red edge” of chlorophyll, which is discussed further below. For gases, a distinct spectral feature or number of features would identify the presence of a potential biogenic gas and further analysis would deduce a concentration or column abundance of the molecule in an exoplanet atmosphere.

Table 4. Potential biosignature gases and associated information. Shown are absorption band centers or band ranges in the UV-visible to near-infrared (NIR), as well as thermal infrared. Particularly strong bands are marked in bold because of their strength and/or lack of contamination from other gases. Square brackets contain the names of particular bands.

Bio-signature	UV-Visible-NIR band center, μm and (cm^{-1})	Visible-NIR band interval cm^{-1}	Thermal IR spectral band center, μm	Biogenic source	Abiogenic false positive
O ₂	1.58 (6329) 1.27 (7874) 1.06 (9433) 0.76 (13158) 0.69 (14493) 0.63 (15873) 0.175-0.19 [Schumann-Runge]	6300-6350 7700-8050 9350-9400 12850-13200 14300-14600 14750-15900	-	<i>Photosynthesis:</i> splitting of water	Cases of water photo-dissociation and preferential escape of hydrogen, with lack of O ₂ sinks
O ₃	4.74 (2110) 3.3 (3030) 0.45-0.85 [Chappuis] 0.30-0.36 [Huggins] 0.2-0.3 [Hartley]	2000-2300 3000-3100 10600-22600	>15 (rotation), 14.3, 9.6, 8.9, 7.1, 5.8	<i>Photosynthesis:</i> photochemically derived from O ₂	As above
CH ₄	3.3 (3030) 2.20 (4420) 1.66 (6005) <0.145 continuum	2500-3200 4000-4600 5850-6100	6.5, 7.7	<i>Methanogenesis:</i> reduction of CO ₂ with H ₂ , often mediated by degradation of organic matter	Geothermal or primordial methane
N ₂ O	4.5 (2224) 4.06 (2463) 2.87 (3484) 0.15-0.20 0.1809, 0.1455, 0.1291	2100-2300 2100-2800 3300-3500	7.78, 8.5, 16.98	<i>Denitrification:</i> reduction of nitrate with organic matter	Some abiotic sources that don't build up on Earth*; also strong coronal mass injection affecting an N ₂ -CO ₂ atmosphere**
NH ₃	4.3, 3.0 (3337) 2.9 (3444) 2.25, 2, 1.5, 0.93, 0.65, 0.55, 0.195, 0.155	2800-3150	6.1, 10.5	<i>Ammonification:</i> Volatilization of dead or waste organic matter	Non-biogenic, primordial ammonia
(CH ₃) ₂ S	3.3 (2997) 3.4 (2925) 0.205, 0.195, 0.145, 0.118	2900-3100	6.9, 7.5, 9.7	plankton	No significant abiotic sources
CH ₃ Cl	3.3 (3291) 3.4 (2937) 0.175, 0.160, 0.140, 0.122	2900-3100	6.9, 9.8, 13.7	Algae, tropical vegetation	No significant abiotic sources (Keppler <i>et al.</i> 2005)
CH ₃ SH	3.3 (3015) 3.4 (2948) 0.204	2840-3100	6.9, 7.5, 9.3, 14.1	Mercaptogenesis: Methanogenic organisms can create CH ₃ SH	No significant abiotic sources

				instead of CH ₄ if given H ₂ S in place of H ₂ (Moran <i>et al.</i> 2008).	
C ₂ H ₆	3.37 (2969) 3.39 (2954) 3.45 (2896) <0.16	2900-3050	6.8, 12.15	Photochemically derived from CH ₄ , CH ₃ SH, and other biologically-produced organic compounds	Could be derived from geothermal or primordial methane

*N₂O has been generated from ‘chemodenitrification’ whereby nitrite (NO₂⁻) or nitrate (NO₃⁻) reacts with Fe²⁺-containing minerals in brines (Jones *et al.* 2015; Samarkin *et al.* 2010). However, on Earth, the source of natural oxidized nitrogen ultimately comes from nitrifying bacteria or atmospheric chemistry that relies upon oxygen, which comes from photosynthesis. Also N₂O can be released from UV photo-reduction of ammonium nitrate (Rubasinghege *et al.* 2011), where the latter comes from humans as industrial fertilizer.

**Airapetian *et al.* (2016).

The abundance of a potentially biogenic gas can be determined most simply in the UV, visible or near-IR where reflected light dominates over thermal emission from a planetary atmosphere and surface. In this case, the latter can be ignored. For example, ignoring scattering, the one-way zenith optical depth of the O₂ A-band (at 760 nm) is related to O₂ column abundance N_0 (molecules cm⁻²), given an absorption cross-section σ_{760} (cm² molecule⁻¹), by

$$\tau_{760} = \int_0^{\infty} \sigma_{760} n(z) dz \approx \sigma_{760} \int_0^{\infty} n(z) dz = \sigma_{760} N_0 \quad (5)$$

where number density n (molecules cm⁻³) is well mixed over altitude z . For an exoplanet, if starlight passes through the atmosphere and is reflected at the surface, then the total O₂ column in the line of sight, N_0 , at the center of the disk is less than the amount N seen by an external observer of the entire exoplanet disk according to an ‘‘effective airmass’’ correction, defined as

$$M^* = N / N_0 \quad (6)$$

Owen (1980) calculated that moderate spectral resolution ($\lambda/\Delta\lambda = 20-100$) could resolve the O₂ A-band on a planet with a level of O₂ the same as the modern Earth, assuming a value of M^* of 3.14. However, the optimum resolution for observing this band will depend on the noise properties of the system. More recent estimates suggest that lower-noise instruments can detect this band with spectral resolutions ~ 150 (Brandt and Spiegel 2014).

In the general case, an effective airmass will depend on an exoplanet’s phase (e.g., full or quarter disk illumination) and the way brightness varies across the disk. Traditionally, one could deduce abundances using the equivalent width, W , of a spectral band,

$$W \propto (\sigma_v N_0 M^* \Delta\nu_L)^n \quad (7)$$

where $\Delta\nu_L$ is the line width and n takes values from end-members of $n = 1$ (weak lines) to $n \sim 0$ (line saturation just beginning) to $n = 1/2$ (strong lines). If unsaturated and saturated lines of a constituent are measured, ‘‘curve of growth’’ laboratory data can be used to find the column abundance of the gas, N_0 . In principle, if the line width $\Delta\nu_L$ comes from pressure-broadening, then, assuming the temperature T is known or can be estimated, one can calculate a total pressure p and a volume mixing ratio of a biosignature gas, $c_i = p_i/p$ where p_i is the partial pressure of the absorbing gas, given by:

$$p_i = n_i kT = \frac{N_0}{H} kT \quad (8)$$

Here, H is the scale height, which will be the same for the constituent as the bulk atmosphere if it is well mixed.

In a more modern treatment, we know enough about the spectral structure of bands to account for line saturation and overlap explicitly to determine gas abundances from spectrum of multiple lines, if present. Thus, iterative procedures would fit a spectrum to a line or multiple lines to estimate the gas abundance(s) if the spectral resolution and signal-to-noise are sufficient.

At longer wavelengths, where thermal emission by the surface and atmosphere dominates over reflected light, the shape of strong absorption bands of vertically well-mixed gases (such as CO₂ for an Earth-like world) makes it possible to determine the temperature structure and retrieve the abundances of gases from altitude- and temperature-dependent IR emission contributions (weighting functions), as mentioned in Sec. 3.3.2.

Techniques for detecting the gaseous components of an atmosphere and the structure of the atmosphere have been demonstrated on larger, uninhabitable planets (Barstow *et al.* 2013; Benneke and Seager 2012; Feng *et al.* 2016; Lee *et al.* 2013; Line *et al.* 2014; Line *et al.* 2013; Line and Yung 2013; Rocchetto *et al.* 2016; Waldmann *et al.* 2015). Similar retrievals are being considered for the search for biosignatures on Earth-like worlds (Barstow *et al.* 2016; Barstow and Irwin 2016). Below, we discuss the need for more even more sophisticated forms of forward and inverse models that link the atmosphere to the potential biogeochemistry of the planet and associated biosignature metrics.

Potential Surface biosignatures

Table 5. Surface biosignatures and related information.

Bio-signature	Visible-NIR band center, μm	Visible-NIR band interval, cm^{-1}	Biogenic source	Abiogenic false positive
Terrestrial vegetation red-edge	0.67-0.76 (a sharp slope between visible absorbance and NIR scattering)	14925-13160	<i>Photosynthesis</i> : “red edge” due to sharp lack of absorption in the NIR by Chlorophyll <i>a</i>	None on Earth
Carotenoids, retinal and other biological pigments	0.40-0.50, 0.53-0.63 and absorption over other narrow wavelength ranges	-Aromatic C-H 3000-3000 -Schiff base compounds (i.e., R ₂ C=NR' (R' ≠ H)) 1620-1700 and others	Photoprotective, phototrophic, or photoreactive and accessory pigments	Future research
Chirality/circular polarization	Dependent on pigment	-	Biological cell molecular structure	Future research

In addition to atmospheric biosignatures, some organisms produce pigments with characteristic spectral reflectance features. Such spectral signatures could increase the confidence of the discovery of life on exoplanets. As described by Schwieterman *et al.*, *this issue*, on Earth, the photosynthetic “red edge” is recognized as a globally detectable signature of life. The red edge is a

sharp slope of increased reflectance in the visible to the near-IR part of the spectrum, $\sim 0.67\text{-}0.76\ \mu\text{m}$ (Sagan *et al.* 1993; Seager *et al.* 2005). This particular biosignature also exhibits strong temporal variability due to seasonal changes in vegetation distribution and density, adding further observational potential (Schwieterman *et al.* 2015a).

The vegetation red-edge remains the only well-accepted surface biosignature. The red edge is caused by red absorbance by chlorophyll *a* in plant leaves and scattering in the NIR where the pigment does not absorb. The red edge is caused by strong absorption of red light by chlorophyll *a* in plant leaves and scattering in the NIR where the pigment does not absorb. The red edge is an expression of light harvesting for photosynthesis as well as of the structure of the host organism (see Schwieterman *et al.*, *this issue*). Among phototrophs, the red edge is not unique in expressing these functions but it is widespread over Earth's surface and lacks any strong false positives for life. Earth-observing satellites quantify the red-edge through measurements of the contrast in between visible and near-IR spectral regions. The most popular is the *normalized difference vegetation index* (NDVI) = $(R_{\text{NIR}} - R_{\text{RED}}) / (R_{\text{NIR}} + R_{\text{RED}})$ (Huete *et al.* 1994; Myneni *et al.* 1995; Myneni *et al.* 1997; Tucker *et al.* 2005), where R_{RED} is the surface reflectance in the red, and R_{NIR} is the reflectance in the near-IR. The red and NIR bands used for NDVI calculations can vary according to satellite sensor design. Precisely designed sensor bands avoid the range 700-760 nm where the red edge is steep, and target adjacent red and NIR bands to measure the strongest contrast in reflectance. For the red, the band is best centered around 650-680 nm where there is a peak in pigment absorbance. The Earth observing satellites Moderate Resolution Imaging Spectrometer (MODIS) and the Landsat Thematic Mapper (TM), which were designed to map vegetation, use a red band spanning 630-690 nm. The index may also sometimes be calculated using a broadband visible (400-700 nm) absorbance in place of the red, since plants harvest light across the visible. For the NIR band, plant leaves have an NIR reflectance plateau across $\sim 760\text{-}1100\ \text{nm}$; however, this range is also impacted by water absorbance bands. MODIS and Landsat TM precisely target a 780-900 nm NIR band to avoid overlap with the red edge and with water.

In an exoplanet observation, the red edge signal strength through an atmosphere will not necessarily be corrected for in telescopic observations of a disk average planetary radiance spectrum. Arnold *et al.* (2008) investigated the red edge in the Earthshine defining an index $\text{VRE} = (R_{\text{NIR}} - R_{\text{RED}}) / R_{\text{RED}}$, which provided a simple measure of the NIR reflectance bump in absence of atmospheric correction. (VRE is not a standard index in vegetation remote sensing and Arnold *et al.* used the reflectance in a narrow near-IR spectral range (740-800 nm) for R_{NIR} and reflectance in a narrow red band (600-670 nm) for R_{RED}). They found that the red-edge detectability ranged from 1% to 12% in observations and models. For a space-based telescope like the Terrestrial Planet Finder/Darwin concepts, the exposure times would be ~ 100 hours to reach a sufficient spectral precision ($< 3\%$) with a spectral resolution ($\lambda/\Delta\lambda$) of 25 for an Earth at 10 parsecs distance (Arnold *et al.* 2002). If detected, seasonal variations may be especially informative.

Besides the red edge, life produces a great diversity of pigments for many biological functions, from phototrophic light-driven transmembrane proton translocation, to photoreactive, phototactic, photoprotective and photorepair systems, respiration components, and photosynthetic reaction centers (Schwieterman *et al.* 2015a). These can vary from the UV to the near infrared (0.1-2.5 μm). Pigments that absorb in the visible region include, for example, cytochromes ($\sim 0.40\ \mu\text{m}$), carotenoids (0.28-0.55 μm), cyanobacterial and chloroplast accessory pigments (0.40-0.74 μm),

bacteriochlorophyll pigments (0.74-1.03 μm), and retinal pigments (0.53-0.63 μm) (DasSarma 2006; Hegde *et al.* 2015). Moreover, chlorophyll pigments have recently been discovered in cyanobacteria, tuned to absorb in the far-red/NIR as long $\sim 0.77 \mu\text{m}$ (Chen 2014; Li and Chen 2015). Biogenic surface spectral features are also the result of ecological signaling (Schwieterman *et al.* 2015a), community signatures (Parenteau *et al.* 2015), chiral molecules (Sparks *et al.* 2012; Sparks *et al.* 2009), and the bidirectional reflectance distribution function (BRDF) that accounts for angle-dependent reflectivity (Doughty and Wolf 2010). On Earth, many of these biological surface features may not be widespread but can be detectable in local remote sensing data. Whether any of these features could dominate on a global scale on an exoplanet remains an open question.

There are multiple issues that remain to be addressed for red-edge and similar biosignatures. 1) Could a similar biosignature appear in another wavelength range because of adaptation to a different spectrum of energy from the host star, or is the wavelength of the red-edge feature constrained by molecular limits? For example, could oxygenic photosynthesis be excluded on exoplanets orbiting very cool M dwarf stars because the star's output is mainly the near-IR, which excites vibrational transitions rather than the electronic ones needed for photosynthesis? 2) If such features exist, what are their false positives? While there are no known false positives for the red-edge, it may be that a similar feature at a different wavelength could have false positives from mineral features. There is not yet a consensus on why the vegetation red edge is red, although some argue that chlorophyll-*a* evolved to exploit the large number of photons in the red part of the Sun's spectrum convolved with the free energy that each converted photon contributes (Bjorn 1976; Björn and Ghiradella 2015; Marosvolgyi and van Gorkom 2010; Milo 2009). 3) If a different pigment signature emerged on another planet, would it also be unique? Clearly, pigments whose role is light harvesting and screening of ionizing radiation or excess light must have a spectral absorbance that is a function of the available light. However, the prominent wavelength bands will depend on molecular energy transduction constraints and the efficiency of the organism, which results from contingent evolutionary pathways, including competitive survival strategies. Also, the color of some pigments can adapt in real time to fluctuating colors of light (Kehoe and Gutu 2006). The colors of other pigments may be fortuitous without a clear function with respect to light interactions. Often, many of these pigments, like carotenoids in halophilic Archaea, may be expressed in response to environmental chemistry, such as oxygen concentration or pH, in addition to light intensities (Slonczewski *et al.* 2010). Moreover, some pigments may be stratified and tuned depending on the environmental conditions, which may lead to their diversity.

A quantitative framework for evaluating surface biosignatures is still at an early stage. Pigments and other biotic surface features might serve as useful biosignatures for increasing the confidence of potential remote detection of life, particularly in cases where biogenic gases are clearly present or even when they are ambiguous. The possible adaptations of a red-edge-like signature and evaluating other pigments and surface biological features as potential biosignatures serve as motivating cases for developing a framework for identifying biosignatures that are functions of their environmental context (Walker *et al.*, *this issue*). Except for chirality and the vegetation red edge, the uniqueness of the other surface spectral signatures and potential for false positives has yet to be scrutinized.

Given the environmental context are detected species conceivably biogenic?

If a candidate biosignature is detected, a variety of corroborating observations can be considered to strengthen or weaken the possibility that life has been found. We expand on two types of corroboration: if the planetary environment and atmospheric environment are conducive to life, and/or if there is direct, supporting evidence of biology itself.

(i) *Does the planetary environment and atmospheric environment support a biological source?*

Future detection of a possible biosignature gas will be much more convincing if corroborating evidence suggests that the exoplanet is likely to support biology, especially a metabolism that generates the biosignature.

The most fundamental evidence supporting inhabitation on a planet from which a potential biosignature gas has been detected would be a surface emission temperature, T_{surfc} , that allows stable liquid water. Alternatively (or additionally), the inference of surficial liquid water could come from abundant H₂O vapor lines in the spectrum, evidence of glint, or polarized reflected light (discussed in Sec. 3.3.2 above). Color variations on a rotating planet might provide circumstantial supporting evidence.

Further environmental corroboration would be the presence of potential substrates or side-products for metabolisms that are being proposed as responsible for a biosignature gas. On an oxidized world, photosynthesis requires CO₂ as a chemical substrate, so detection of CO₂ would support the possibility that O₂ is a biosignature. Biological denitrification produces N₂O, but (on Earth, at least) it also produces even more N₂, so that the presence of the two gases together would strengthen the idea that N₂O is biological.

The presence of a biosignature gas should also be accompanied by its expected photochemical products. For example, the detection of O₂ would be corroborated by the detection of O₃ (ozone) in the atmosphere because O₃ is derived from O₂ through photochemical reactions, if the star produces adequate near-UV flux. Such pairs of detections can also be used to help constrain the concentration of a gas – for example, the O₃ amount is non-linearly dependent on the O₂ concentration (Kasting *et al.* 1985).

The mixture of gases in an atmosphere could also be more or less consistent with biology, and with the biosignature that has been detected. If a biosphere modulates the composition of a planetary atmosphere, then it will tend to remove gases that are easy to metabolize. In a reducing atmosphere analogous to the atmosphere of the Archean Earth on an inhabited planet, we would not expect H₂ to attain a high abundance in the presence of CO₂ because these two substances can be readily used as metabolic reactants to produce CH₄ via the methanogenesis pathway, $\text{CO}_2 + 4\text{H}_2 \rightarrow \text{CH}_4 + 2\text{H}_2\text{O}$. Lab experiments and bioenergetic calculations show that >90% of the hydrogen is converted to methane if CO₂ is not limiting (Kasting *et al.* 2001; Kral *et al.* 1998). In addition, if CH₄:CO₂ ratios exceed ~0.1, and there is adequate UV flux from the star, an organic haze is produced (Arney *et al.* 2016; Haqq-Misra *et al.* 2008; Trainer *et al.* 2006), which may decrease biological productivity through an anti-greenhouse effect on the climate (Haqq-Misra *et al.* 2008). Thus, if the concentration ratio of CO₂:CH₄:H₂ consists of a sequence of sharply declining numbers, it would be consistent with the presence of biosphere in which methanogenesis is converting CO₂ and H₂ into CH₄. On the other hand, a small amount of CH₄ in a hydrogen-rich atmosphere (a high H₂:CH₄ ratio) could result from abiotic chemistry, and the interpretation of CH₄ as a biosignature would thus be suspect. Similar

arguments have been made on the limits to life within the Solar System, on both Enceladus (Waite *et al.* 2017) and Mars (Sholes *et al.* 2017).

Finally, if there is enough information about the atmospheric composition and planetary environment, it may be possible to assess the magnitude of atmospheric chemical disequilibrium. On Earth, large biogenic fluxes of gases from different ecosystems produce mixtures of gases that are chemically unstable on long timescales (Lovelock 1965; Lovelock 1975). A methodology for quantification of thermodynamic chemical disequilibrium has been established and could be applied (Krissansen-Totton *et al.* 2016a). To calculate chemical disequilibrium properly for an Exo-Earth one must consider all fluid phases because the largest source of disequilibrium in Earth's atmosphere-ocean system is attributable to the coexistence of N₂, O₂, and liquid water (Krissansen-Totton *et al.* 2016a). This disequilibrium is biogenic because current levels both atmospheric N₂ and O₂ are replenished by biological processes and would not persist in the absence of life. For an exoplanet, detecting such multiphase disequilibria would require knowledge that an extensive liquid ocean exists using the techniques described in section 3.3.2.

If just gaseous components are known for an exoplanet, it may be possible to estimate their kinetic instability, i.e., residence time against photochemical destruction, and deduce whether a large, potentially biogenic source is needed. A short lifetime (~10 years) and an inferred large flux into the atmosphere is the case for CH₄ in Earth's O₂-rich atmosphere.

For biological pigments, the planet's environment may help predict the presence of a pigment due to its function. For example, light-harvesting pigments should absorb at wavelengths where there is available light and with sufficient energy per photon to perform the necessary tasks of charge separation or proton pumping (Kiang *et al.* 2007; Stomp *et al.* 2007). Bacteria such as the radiotolerant *Deinococcus radiodurans* manufacture anti-oxidant carotenoids, such as deinoxanthin, in response to UV, and extraterrestrial microbe-like life may have similar physiological response (Tian and Hua 2010). Meanwhile, some biological pigments have colors that are fortuitous and unrelated to the light environment, but may be a function of the chemical environment, such as pH (Slonczewski *et al.* 2010). Since organisms can have more than one strategy for survival, and we cannot measure environmental variables like pH remotely, constraining the suitable environments for these alternative biosignatures is a matter of more research.

(ii) *Are there corroborating biosignatures?*

If a biosignature is detected, direct corroborating evidence could take the form of either evidence of the biogenic source of that biosignature or there could be another, independent biosignature suggesting the presence of biology that is not directly related to the other biosignature. Examples of these are as follows:

(a) Corroborating evidence of a biogenic source.

If H₂O and O₂ have been detected, an additional corroborating biosignature would be the red-edge of a pigment that is widespread on the planet and essential to the function of photosynthetic production of O₂. Also, the presence of biogenic N₂O would be consistent with oxygenic photosynthesis because it derives from abundant organic matter produced from photosynthesis and oxidized forms of nitrogen. The latter include nitrate (NO₃⁻) or nitrite (NO₂⁻) that form in the presence of O₂ when ammonium (NH₄⁺) derived from organic matter is oxidized. Another possibility might be seasonal trends

consistent with biology. For example, detection of seasonal variations of a potentially biogenic gas (CH₄), substrate for photosynthesis (CO₂), or pigment could be corroborative.

(b) Another, not necessarily directly corroborative, biosignature.

If O₂ has been detected, the presence of CH₄ would be an example of an independent biosignature, given that CH₄ is not expected to be abundant in an O₂ atmosphere unless there is a significant source, such as methanogenesis. The simultaneous detection of O₂ and CH₄ would constitute a very compelling biosignature because of the short photochemical lifetime of CH₄ in oxidizing atmospheres, as described above.

The need for chemical-radiative forward models and retrievals of atmospheric composition

The above discussion indicates the obvious need to understand the biogeochemistry of exoplanets in order to interpret biosignatures. Of course, there is still considerable work to be done to understand the co-evolution of biogeochemical cycles and atmospheric composition on Earth, which is being done using “Earth System” models. Such models are corroborated through geochemical and isotopic paleoclimate proxies over geologic time (Berner 2004; Kump *et al.* 2010; Langmuir and Broecker 2012; Mackenzie and Lerman 2006).

For exoplanets, we conceive of “Exo-Earth System” models, as mentioned earlier. These would couple a surface biosphere to atmospheric chemistry and climate. The latter would necessarily use radiative transfer and models could also include atmospheric and ocean dynamics. A model could also include how the interior thermal evolution of a planet couples to mantle processes and surface outgassing through volcanic and metamorphic gases. Ultimately, such forward models would be used to generate a synthetic reflectance or transmission spectrum. Hitherto, such spectra have been generated for more specific cases that use Earth-like exoplanet atmosphere models rather than Exo-Earth System models, *per se* (e.g., Arney *et al.* 2016; Robinson *et al.* 2011).

In the future, an Exo-Earth System model might be configured in the form of an inverse fit to spectra from exoplanets. If data had sufficient fidelity, a Bayesian fit would allow for quantitative constraints on possible gas fluxes that are needed to support a potential biosignature gas. An investigation of covariance of uncertain parameters in such a fit would show which parameters we need to know better from future observations to improve confidence that the spectrum really represents biology. For example, a better constraint of one particular parameter could remove degeneracies (i.e., where two or parameters have similar overall effects) and produce a better model fit to the spectrum. Such parameters could be particular environmental constraints or atmospheric gas abundances, for example. Further discussion of models and development we need in the area of biosignatures is given in Walker *et al.* (*this issue*).

3.4. Component 4: Excluding explicit false positives

There are situations where a molecule is predominantly biogenic on Earth but could be an abiotic species on an exoplanet, as noted in **Table 4**. For example, as described by Meadows *et al.* [*this issue*], several theoretical studies have shown that abiotic, bulk O₂ could be present under certain hypothesized circumstances. Specifically, oceans are hypothesized to vaporize and be lost from habitable zone planets in the luminous pre-main sequence phases of M dwarfs, leaving behind very O₂-rich atmospheres (Luger and Barnes 2015). There are some skeptics of such ideas, however, e.g., see discussion in Zahnle and Catling (2017). The extent to which such purely theoretical ideas are

realized remains to be determined, but their possibility demands caution. Meadows *et al.* [*this issue*] describe the potential observational diagnosis of various hypotheses of abiotic O₂.

A general process for excluding false positives of biogenic processes might include the following components: First, it is necessary to identify a plausible abiotic source. Second, the abiotic source must be detected or corroborating evidence to support an abiotic source must be identified. We expand on these concepts, as follows.

(a) *Are there abiotic sources and scenarios where the abiotic source could dominate?*

Considerable research has been devoted to identifying abiotic sources of O₂ and its photochemical product O₃ (Domagal-Goldman *et al.* 2014; Gao *et al.* 2015; Harman *et al.* 2015; Tian *et al.* 2014). However, relatively little attention has been given to abiotic scenarios where other candidate biosignature gases could be significant. In general, the following processes could cause abiotic sources of gases:

(i) Photochemistry and atmospheric-loss processes (including escape-enhanced gases).

For example, in a dry CO₂-rich atmosphere, O₂ could potentially build up from photochemical destruction of CO₂ (Gao *et al.* 2015). It has also been proposed that O₂ could build up abiotically on highly irradiated planets as a result of escape of hydrogen from water photolysis (Luger and Barnes 2015).

(ii) Geothermal (volcanic, metamorphic, geomorphological).

Methane is an example of a biogenic gas that may have abiotic sources. Nearly all CH₄ on Earth has a direct biogenic source or comes indirectly from biology via thermal breakdown of old organic matter, but some argue that CH₄ can be produced abiotically. The geological process of serpentinization produces H₂ when liquid H₂O oxidizes iron in rocks. Fischer-Tropsch reactions could cause subsequent abiotic reduction of inorganic carbon into methane and other abiotic organic compounds (Berndt *et al.* 1996; Etiope and Lollar 2013). However, some recent laboratory simulations of serpentinization have produced no detectable CH₄ (Grozeva *et al.* 2017; McCollom and Donaldson 2016), suggesting that CH₄ may have arisen in earlier experiments from organic contamination (McCollom 2016). Thus, how much CH₄ can be produced abiotically on an exoplanet as a false positive remains a matter of research.

(iii) Impact delivery

Impacts that have reducing chemistry in the impact plume could generate substantial amounts of abiotic CH₄ and NH₃ (Zahnle *et al.* 2010), which are potential false positives.

(iv) Surface signatures: Mineral spectra or other spectral contaminants.

Cautionary tales of spectral contaminants are the false spectral detection of vegetation and methane on Mars in the 1950s-1960s. Spectral features near 3.5 μm (which became known as “Sinton bands”) were detected by ground-based telescopes and erroneously attributed to vegetation due to similarity with lichen spectra (Sinton 1957; Sinton 1959). Subsequent work showed that the Sinton bands were due to terrestrial HDO (Rea *et al.* 1965). Similarly, initial reports of ammonia and methane in the near-IR reflection spectrum of the polar caps of Mars observed by the Mariner 7 flyby were subsequently shown to be due to solid CO₂ at the surface (Herr and Pimentel 1969).

(v) Spectral contamination by a moon (or a parent planet if the target body is a moon).

When an exoplanet hosts a moon with its own atmosphere, a single spectrum that includes both moon and exoplanet could end up resembling a mixture of both atmospheres and thus perhaps chemical disequilibrium false positives (Rein *et al.* 2014).

(vi) Mass loss processes

Potentially, one could conceive of exoplanets that lose mass from their surfaces in a way that resembles the input of biogenic gas. For example, clathrates in cold regions could melt and input methane into an atmosphere. Another example is unexpectedly abundant molecular oxygen that was found in the coma of comet 67P/Churyumov-Gerasimenko. Here, O₂ may be formed abiotically by collision of energetic water ions with oxygen-containing minerals on the comet's surface (Yao and Giapis 2017).

(b) Find corroborating evidence to support an abiotic source

In general, an abiotic source of a biosignature tends to occur under pathological circumstances and so should be accompanied by diagnostic photometric features associated with those hypothesized conditions. In the proposed cases of abiotic oxygen, various diagnostics have been deduced (Schwieterman *et al.* 2016) (see also Meadows *et al.*, this issue). If O₂ builds up on a dry planet from CO₂ photolysis (Gao *et al.* 2015), the dryness and presence of CO are diagnostics. A proposed build up of tens or hundreds of bars of pO₂ on planets around M stars because of a runaway greenhouse during pre-main sequence super-luminous phase (Luger and Barnes 2015), if real (Zahnle and Catling 2017), would be indicated by a strong O₄ dimer feature. Hypothetical planets that lack non-condensable N₂ and build up O₂ from water vapor destruction and loss (Wordsworth and Pierrehumbert 2014) would also have strong O₄ and lack the N₄ dimer signatures. Similarly, in cases of O₂ or O₃ photochemical build-up on M-star planets (Domagal-Goldman *et al.* 2014; Tian *et al.* 2014), if real (Harman *et al.* 2015), a lack of CH₄ would be expected. Similar diagnostics for other potential false positives are expected and remain to be investigated.

After gathering information pertinent to all four framework components in **Figure 2**, it is likely that follow-up observations would be required, i.e., gaining further observations relevant to components 1-4 as necessary. The exact procedure would be defined by the specific scenario and suite of observations existing at the time, which is a matter for future observers, so we do not comment further.

4. A proposed system of confidence levels of life detection on exoplanets

Table 6. Possible categories for probability of life detection on individual exoplanets. Examples are illustrative and based on current thinking in the field. In reality, specific exoplanet cases would have to be quantified by calculating a Bayesian posterior probability to determine the exact level.

Confidence level for detection of life	Posterior Probability $P(\text{life} \text{data, context})$	Evidence	Possible but purely illustrative examples
Level 1: Very likely inhabited	90-100%	Multiple lines of evidence for life. Given current understanding of planetary processes, no known abiotic process can plausibly explain all observed features.	An O ₂ -rich atmosphere with other biosignature gases, including CH ₄ and N ₂ O, and a liquid ocean identified on an Earth-size exoplanet in the habitable zone.

<i>Level 2:</i> Likely inhabited	66-100%	The body of evidence is consistent with the presence of life.	Atmospheric O ₂ detected together with CO ₂ and water vapor on an exoplanet in the habitable zone.
<i>Level 3:</i> About as likely as not inhabited (inconclusive)	33–66%	Some evidence for life, but insufficient contextual information to draw a definitive conclusion because plausible alternative abiotic explanations cannot be ruled out.	O ₂ detection in isolation; or an organic haze with abundant CH ₄ ; or pigment-like biosignatures; or N ₂ -CO ₂ atmosphere. Circumstantial evidence for liquid water.
<i>Level 4:</i> Likely uninhabited	0-33%	Observational evidence that the planet is habitable, but no biosignatures detected despite an exhaustive search.	Planet is in the habitable zone and has an atmosphere with abundant water vapor features. But no biosignatures are detected despite extensive data.
<i>Level 5:</i> Very likely uninhabited	0-10%	Criteria for habitability are not met or atmospheric anti-biosignatures are detected.	CO ₂ -rich, desiccated planets; or CO ₂ -H ₂ anti-biosignature atmosphere; or abundant CO anti-biosignature

The proposed biosignature assessment framework (**Figures 1 and 2**) ultimately should produce posterior probabilities for the presence of life on an exoplanet, which can be tied to a system of qualitative descriptions for the confidence of life detection. Similar ideas have been used in other scientific areas. For example, global warming is described in such terms in reports of the Intergovernmental Panel on Climate Change (IPCC). Their set of levels are: very likely 90–100%, likely 66–100%, about as likely as not 33–66%, unlikely 0–33%, and very unlikely 0–10% (Stocker *et al.* 2013).

We follow the IPCC example and suggest five levels of confidence in reporting the possible presence of life on exoplanets (**Table 6**). A “*Level 1*” detection of a *very likely inhabited* exoplanet requires multiple lines of evidence and a posterior probability of life being present of 90-100%, given the data and context. For example, a habitable zone planet very similar to Earth with coexisting atmospheric O₂, CH₄, N₂O, and CO₂, along with evidence of liquid water ocean, might fall into this category because an abiotic system would be very unlikely to mimic all of those data. A *likely inhabited* “*Level 2*” detection (66-100% posterior probability) would have consistency with the presence of life. For example, an O₂-rich atmosphere with a pigment-like spectrum – with no further information -- would be suggestive of life, but not as definitive as Level 1, and might qualify for Level 2. A “*Level 3*” detection (33-66% posterior probability) would be inconclusive, and essentially equivalent to a weaker statement of “maybe but we don’t know”. A detection of O₂ in isolation might only be a Level 3 detection in this assessment, where some possible alternative abiotic scenarios cannot be ruled out. A “*Level 4*” detection of an *unlikely* inhabitation would require a lack of biosignature detection even though some data allow the planet to be habitable in principle, e.g., a planet in the habitable zone with an atmosphere but no detection of biosignatures despite an extensive search. Finally, “*Level 5*” planets would have direct evidence that rule out their habitability and render them very unlikely to be inhabited. For example, the exoplanet might be dry with an atmosphere dominated by CO₂. Alternatively, the planet might have the presence of anti-biosignatures. However, Level 5 “dead” planets will be extremely important for understanding the prevalence of life by building up statistics.

5. Conclusions

We have presented a general scheme for observing potential exoplanet biosignatures and determining confidence levels for positive detection of signs of life or making a more rigorous assessment that life has not been found (**Figure 1**). The framework uses models of planetary atmospheres and

environments with spectral or photometric data that contain potential biosignatures to find the Bayesian likelihoods of those data occurring if the exoplanet has or does not have life. The latter includes “false positives” where abiotic sources mimic biosignatures. Prior knowledge (including all factors that influence habitability and previous exoplanet observations) gives a prior probability of life being present on a potentially habitable exoplanet. The likelihood of data occurring in the presence or absence of life is weighted by the prior probability. The result is a Bayesian posterior probability of life existing on a given exoplanet given the observations.

Within this framework, we outlined four observational and analytical components to determine whether biosignatures truly represent the presence of life, which are intended to be iterative, i.e., knowledge from some components can be improved or expanded with subsequent observations and models if biosignatures are suspected. The components (shown in **Figure 2**) are as follows:

- 1) Characterize the stellar properties and exoplanetary system properties to determine whether the planet is in a stable habitable zone. Stellar parameters, e.g., age and spectrum, provide context for interpreting potential biosignatures. The orbital parameters of the exoplanetary system and “external” parameters of the exoplanet itself (e.g., mass and radius) are required. Properties that are desirable or essential for this component of the framework are tabulated in **Table 1**.
- 2) Characterize the exoplanet surface and atmosphere to determine whether the surface environment is potentially habitable. These include the thermal emittance and Bond albedo, which are needed to estimate the surface temperature (i.e., whether liquid water is stable on the surface) as opposed to merely being in a habitable zone. Such “internal” properties of an exoplanet that are desirable or essential for this component are tabulated in **Tables 2**, while spectral bands for atmospheric composition are tabulated in **Table 3**.
- 3) Search for potential biosignatures in the available data. Most biosignatures consist of spectral evidence of a biogenic gas (**Table 4**) and a deduction of its concentration or column abundance in an exoplanet atmosphere. Pigments and surface biosignatures (**Table 5**) represent potentially confirmatory biosignatures increasing the confidence of remote detection of life. The biogenic nature of such molecules must be assessed through the environmental context deduced through components 1-2 and also any corroborating evidence such as other information on atmospheric composition. Models of atmospheric composition and climate are an important part of such an assessment. Covariances of parameters identified in inverse modeling with a chemical-radiative atmospheric forward model would help prioritize which parameters are most important for follow-up observations.
- 4) Exclude false positives. Coupled geochemical-climate “Exo-Earth System” models would be used to simulate the interconnected parts of an Earth-like planet, such as the interior (e.g., mantle thermal evolution), ocean, biosphere, and atmosphere. Critically, Exo-Earth models must be developed that generate synthetic exoplanet spectra or photometric data to estimate the likelihoods of the data occurring in either the presence or absence of life.

Finally, we outlined how Bayesian posterior probabilities of life detection from the proposed framework would map to scheme of five confidence levels for announcing the results of searches for life on exoplanets (**Table 6**). With decreasing confidence, these levels are “very likely”, “likely”, “inconclusive”, “unlikely”, and “very unlikely” inhabited. We discussed possible criteria that would determine whether an analysis of future data would fall into a particular level. Ultimately, the Bayesian posterior probability would determine the level.

Appendix A: Bayesian formalism

Bayes' theorem, in its standard simple form, is:

$$P(\text{hypothesis} | \text{evidence}) = \frac{P(\text{evidence} | \text{hypothesis})}{\underbrace{P(\text{evidence})}_{\text{support the evidence provides for the hypothesis}}} \times \underbrace{P(\text{hypothesis})}_{\text{the prior}} \quad (\text{A1})$$

Here, one reads “hypothesis” as the “hypothesis being true” and the P 's are probabilities. The theorem gives $P(\text{hypothesis} | \text{evidence})$, the probability of the hypothesis being true given the evidence, as a function of the likelihood of the evidence occurring if the hypothesis is true, $P(\text{evidence} | \text{hypothesis})$ divided by a marginal likelihood, $P(\text{evidence})$. The ratio on the right-hand side is weighted by a prior probability for the hypothesis being true, $P(\text{hypothesis})$.

In the case of a binary hypothesis that is either true or false, and $P(\text{evidence}) > 0$, an extended version of Bayes theorem is:

$$P(\text{hypothesis} | \text{evidence}) = \frac{P(\text{evidence} | \text{hypothesis})P(\text{hypothesis})}{P(\text{evidence} | \text{hypothesis})P(\text{hypothesis}) + P(\text{evidence} | \text{hypothesis false})P(\text{hypothesis false})} \quad (\text{A2})$$

This form of Bayes' theorem is the one used in this paper.

We make the extended Bayes' theorem specific to the case of the hypothesis of life existing on an exoplanet. Then, the posterior probability we seek is $P(\text{life} | \text{data}, \text{context})$, which is the probability of life on an exoplanet given spectral or photometric ‘data’ of the exoplanet and the ‘context’, which consists of all the known exoplanet system or stellar properties. By Bayes' extended theorem, eq. (A2), and the rules of conditional probability, we have

$$\begin{aligned} P(\text{life} | \text{data}, \text{context}) &= \frac{P(\text{data}, \text{context} | \text{life})P(\text{life})}{P(\text{data}, \text{context} | \text{life})P(\text{life}) + P(\text{data}, \text{context} | \text{no life})P(\text{no life})} \\ &= \frac{P(\text{data} | \text{context}, \text{life})P(\text{context} | \text{life})P(\text{life})}{P(\text{data} | \text{context}, \text{life})P(\text{context} | \text{life})P(\text{life}) + P(\text{data} | \text{context}, \text{no life})P(\text{context} | \text{no life})P(\text{no life})} \end{aligned} \quad (\text{A3})$$

The probability of the contextual information about the exoplanet (e.g., its mass and radius) and star (e.g., the spectral energy distribution from the star) is independent of whether there is life on the exoplanet in question. Thus,

$$P(\text{context} | \text{no life}) = P(\text{context} | \text{life}) \quad (\text{A4})$$

Consequently, those terms cancel out in eq. (A3) to give eq. (1) in the main text.

Acknowledgements

DCC, DC, NYK, and SD-G were supported to do this work by NASA Astrobiology Institute's Virtual Planetary Laboratory under Cooperative Agreement Number NNA13AA93A. JKT was supported by NASA Earth and Space Sciences Fellowship NNX15AR63H.

References.

Airapetian V. S., Glöcer A., Gronoff G., Hebrard E., and Danchi W. (2016) Prebiotic chemistry and atmospheric warming of early Earth by an active young Sun. *Nature Geosci.*, 9: 452-455.

- Armstrong J. C., Barnes R., Domagal-Goldman S., Breiner J., Quinn T. R., and Meadows V. S. (2014) Effects of extreme obliquity variations on the habitability of exoplanets. *Astrobiology*, 14: 277-291.
- Arney G., Domagal-Goldman S. D., Meadows V. S., Wolf E. T., Schwieterman E., Charnay B., Claire M., Hébrard E., and Trainer M. G. (2016) The Pale Orange Dot: The spectrum and habitability of hazy Archean Earth. *Astrobiology*, 16: 873-899.
- Arnold L. (2008) Earthshine observation of vegetation and implication for life detection on other planets: A review of 2001–2006 works. *Space Sci. Rev.*, 135: 323-333.
- Arnold L., Gillet S., Lardiere O., Riaud P., and Schneider J. (2002) A test for the search for life on extrasolar planets: Looking for the terrestrial vegetation signature in the Earthshine spectrum. *Astron. Astrophys.*, 392: 231-237.
- Barnes R., Mullins K., Goldblatt C., Meadows V. S., Kasting J. F., and Heller R. (2013) Tidal Venuses: Triggering a climate catastrophe via tidal heating. *Astrobiology*, 13: 225-250.
- Barnes R., Raymond S. N., Jackson B., and Greenberg R. (2008) Tides and the evolution of planetary habitability. *Astrobiology*, 8: 557-568.
- Barstow J. K., Aigrain S., Irwin P. G. J., Fletcher L. N., and Lee J. M. (2013) Constraining the atmosphere of GJ 1214b using an optimal estimation technique. *Mon. Not. R. Astron. Soc.*, 434: 2616-2628.
- Barstow J. K., Aigrain S., Irwin P. G. J., Kendrew S., and Fletcher L. N. (2016) Telling twins apart: exo-Earths and Venuses with transit spectroscopy. *Mon. Not. R. Astron. Soc.*, 458: 2657-2666.
- Barstow J. K., and Irwin P. G. J. (2016) Habitable worlds with JWST: transit spectroscopy of the TRAPPIST-1 system? *Mon. Not. R. Astron. Soc.*, 461: L92-L96. doi:10.1093/mnrasl/slw109.
- Batygin K., Bodenheimer P., and Laughlin G. (2009) Determination of the interior structure of transiting planets in multiple-planet systems. *Astrophys. J. Lett.*, 704: L49.
- Batygin K., and Laughlin G. (2011) Resolving the sin(I) degeneracy in low-mass multi-planet systems. *Astrophys. J.*, 730: 95.
- Bazot M., Christensen-Dalsgaard J., Gizon L., and Benomar O. (2016) On the uncertain nature of the core of α Cen A. *Mon. Not. R. Astron. Soc.*, 460: 1254-1269.
- Becker J., C., and Batygin K. (2013) Dynamical measurements of the interior structure of exoplanets. *Astrophys. J.*, 778: 100.
- Benneke B., and Seager S. (2012) Atmospheric retrieval for Super-Earths: Uniquely constraining the atmospheric composition with transmission spectroscopy. *Astrophys. J.*, 753: 100.
- Berndt M. E., Allen D. E., and Seyfried W. E. (1996) Reduction of CO₂ during serpentinization of olivine at 300°C and 500 bar. *Geology*, 24: 351-354.
- Berner R. A. (2004) *The Phanerozoic Carbon Cycle: CO₂ and O₂*. Oxford Univ. Press, Oxford.
- Bjorn L. O. (1976) Why are plants green? Relationships between pigment absorption and photosynthetic efficiency. *Photosynthetica*, 10: 121-129.
- Björn L. O., and Ghiradella H. (2015) Spectral tuning in biology I: Pigments. In: *Photobiology: The Science of Light and Life*. edited by LO Björns, Springer New York, New York, NY, pp 97-117.
- Bond J., C., O'Brien D., P., and Lairetta D., S. (2010) The compositional diversity of extrasolar terrestrial planets. I. In situ simulations. *Astrophys. J.*, 715: 1050.
- Borucki W. J., Dunham E. W., Koch D. G., Cochran W. D., Rose J. D., Cullers D. K., Granados A., and Jenkins J. M. (1996) FRESIP: A mission to determine the character and frequency of extra-solar planets around solar-like stars. *Astrophys. Space Sci.*, 241: 111-134.
- Brandt T. D., and Spiegel D. S. (2014) Prospects for detecting oxygen, water, and chlorophyll on an exo-Earth. *P. Natl. Acad. Sci. USA*, 111: 13278-13283.
- Carter B. (1983) The Anthropoc Principle and its implications for biological evolution. *Phil. Trans. R. Soc. Lond. A*, 310: 347-363.

- Carter-Bond J., C., O'Brien D., P., and Raymond S., N. (2012) The compositional diversity of extrasolar terrestrial planets. II. Migration simulations. *Astrophys. J.*, 760: 44.
- Catling D. C., and Claire M. W. (2005) How Earth's atmosphere evolved to an oxic state: A status report. *Earth Planet. Sci. Lett.*, 237: 1-20.
- Catling D. C., Glein C. R., Zahnle K. J., and McKay C. P. (2005) Why O₂ is required by complex life on habitable planets and the concept of planetary "oxygenation time". *Astrobiology*, 5: 415-438.
- Catling D. C., and Kasting J. F. (2017) Atmospheric Evolution on Inhabited and Lifeless Worlds. Cambridge Univ. Press, New York.
- Chen M. (2014) Chlorophyll modifications and their spectral extension in oxygenic photosynthesis. *Annu. Rev. Biochem.*, 83: 317-340.
- Chyba C. F., and Phillips C. B. (2001) Possible ecosystems and the search for life on Europa. *P. Natl. Acad. Sci. USA*, 98: 801-804.
- Cowan N. B., Agol E., Meadows V. S., Robinson T., Livengood T. A., Deming D., Lisse C. M., A'Hearn M. F., Wellnitz D. D., Seager S. and others. (2009) Alien maps of an ocean-bearing world. *Astrophys. J.*, 700: 915-923.
- DasSarma S. (2006) Extreme halophiles are models for astrobiology. *Microbe*, 1: 120-126.
- David E. M., Quintana E. V., Fatuzzo M., and Adams F. C. (2003) Dynamical stability of Earth-like planetary orbits in binary systems. *Publ. Astron. Soc. Pac.*, 115: 825-836.
- Demory B. O., de Wit J., Lewis N., Fortney J., Zsom A., Seager S., Knutson H., Heng K., Madhusudhan N., Gillon M. and others. (2013) Inference of inhomogeneous clouds in an exoplanet atmosphere. *Astrophys. J. Lett.*, 776: L25.
- Domagal-Goldman S. D., Meadows V. S., Claire M. W., and Kasting J. F. (2011) Using biogenic sulfur gases as remotely detectable biosignatures on anoxic planets. *Astrobiology*, 11: 419-441.
- Domagal-Goldman S. D., Segura A., Claire M. W., Robinson T. D., and Meadows V. S. (2014) Abiotic ozone and oxygen in atmospheres similar to prebiotic Earth. *Astrophys. J.*, 792: doi: 10.1088/0004-637X/792/2/90.
- Doughty C. E., and Wolf A. (2010) Detecting tree-like multicellular life on extrasolar planets. *Astrobiology*, 10: 869-879.
- Drossart P., Rosenqvist J., Encrenaz T., Lellouch E., Carlson R. W., Baines K. H., Weissman P. R., Smythe W. D., Kamp L. W., Taylor F. W. and others. (1993) Earth global mosaic observations with NIMS-Galileo. *Planet. Space Sci.*, 41: 551-561.
- Elser S., Meyer M. R., and Moore B. (2012) On the origin of elemental abundances in the terrestrial planets. *Icarus*, 221: 859-874.
- Encrenaz T. (2014) Infrared spectroscopy of exoplanets: observational constraints. *Philosophical transactions. Series A, Mathematical, physical, and engineering sciences*, 372: 20130083.
- Etioppe G., and Lollar B. S. (2013) Abiotic methane on Earth. *Rev. Geophys.*, 51: 276-299.
- Feng Y. K., Line M., R., Fortney J., J., Stevenson K., B., Bean J., Kreidberg L., and Parmentier V. (2016) The impact of non-uniform thermal structure on the interpretation of exoplanet emission spectra. *Astrophys. J.*, 829: 52.
- Fischer D. A., and Valenti J. (2005) The planet-metallicity correlation. *Astrophys. J.*, 622: 1102-1117.
- Fletcher N. H. (1970) The Chemical Physics of Ice. Cambridge Univ. Press, London.
- Ford E. B., Seager S., and Turner E. L. (2001) Characterization of extrasolar terrestrial planets from diurnal photometric variability. *Nature*, 412: 885-887.
- Fortney J. J. (2005) The effect of condensates on the characterization of transiting planet atmospheres with transmission spectroscopy. *Mon. Not. R. Astron. Soc.*, 364: 649-653.
- Fujii Y., and co-authors. (2017) Exoplanet biosignatures: Observational prospects. *Astrobiol.*: this issue.
- Gaidos E. (2015) What are little worlds made of? Stellar abundances and the building blocks of planets. *Astrophys. J.*, 804: 40.

- Gaidos E., and Williams D. M. (2004) Seasonality on terrestrial extrasolar planets: inferring obliquity and surface conditions from infrared light curves. *New Astron.*, 10: 67-77.
- Gao P., Hu R. Y., Robinson T. D., Li C., and Yung Y. L. (2015) Stability of CO₂ atmospheres on desiccated M-dwarf exoplanets. *Astrophys. J.*, 806: 249.
- Gillon M., Triaud A. H. M. J., Demory B.-O., Jehin E., Agol E., Deck K. M., Lederer S. M., de Wit J., Burdanov A., Ingalls J. G. and others. (2017) Seven temperate terrestrial planets around the nearby ultracool dwarf star TRAPPIST-1. *Nature*, 542: 456-460.
- Goldblatt C. (2016) The inhabitation paradox: How habitability and inhabitancy are inseparable. <https://arxiv.org/abs/1603.00950>.
- Griessmeier J. M., Stadelmann A., Motschmann U., Belisheva N. K., Lammer H., and Biernat H. K. (2005) Cosmic ray impact on extrasolar earth-like planets in close-in habitable zones. *Astrobiology*, 5: 587-603.
- Grozeva N. G., Klein F., Seewald J. S., and Sylva S. P. (2017) Experimental study of carbonate formation in oceanic peridotite. *Geochim. Cosmochim. Acta*, 199: 264-286.
- Haqq-Misra J. D., Domagal-Goldman S. D., Kasting P. J., and Kasting J. F. (2008) A revised, hazy methane greenhouse for the Archean Earth. *Astrobiol.*, 8: 1127-1137.
- Harman C. E., Schwieterman E. W., Schottelkotte J., and Kasting J. F. (2015) Abiotic O₂ levels on planets around F, G, K, and M stars: Possible false positives for life? *Astrophys. J.*: in press.
- Hartogh P., Jarchow C., Lellouch E., de Val-Borro M., Rengel M., Moreno R., Medvedev A., Sagawa H., Swinyard B., Cavalie T. and others. (2010) Herschel/HIFI observations of Mars: First detection of O₂ at submillimetre wavelengths and upper limits on HCl and H₂O₂. *Astron. Astrophys.*, 521.
- Hegde S., Paulino-Lima I. G., Kent R., Kaltenegger L., and Rothschild L. (2015) Surface biosignatures of exo-Earths: Remote detection of extraterrestrial life. *P. Natl. Acad. Sci. USA*, 112: 3886-3891.
- Heller R., and Hippke M. (2017) Deceleration of high-velocity interstellar photon sails into bound orbits at α -Centauri. *Astrophys. J. Lett.*, 835: L32.
- Herr K. C., and Pimentel G. C. (1969) Infrared absorptions near 3 microns recorded over polar cap of Mars. *Science*, 166: 496-499.
- Holland H. D. (2009) Why the atmosphere became oxygenated: A proposal. *Geochim. Cosmochim. Acta*, 73: 5241-5255.
- Howett C. J. A., Spencer J. R., Pearl J., and Segura M. (2010) Thermal inertia and bolometric Bond albedo values for Mimas, Enceladus, Tethys, Dione, Rhea and Iapetus as derived from Cassini/CIRS measurements. *Icarus*, 206: 573-593.
- Hu R. Y., Ehlmann B. L., and Seager S. (2012) Theoretical Spectra of Terrestrial Exoplanet Surfaces. *Astrophysical Journal*, 752.
- Huete A., Justice C., and Liu H. (1994) Development of vegetation and soil indexes for MODIS-EOS. *Remote Sens. Environ.*, 49: 224-234.
- Johnson J. A., Aller K. M., Howard A. W., and Crepp J. R. (2010) Giant planet occurrence in the stellar mass-metallicity plane. *Publ. Astron. Soc. Pac.*, 122: 905-915.
- Jones L. C., Peters B., Pacheco J. S. L., Casciotti K. L., and Fendorf S. (2015) Stable isotopes and iron oxide mineral products as markers of chemodenitrification. *Environ. Sci. & Tech.*, 49: 3444-3452.
- Joshi M. M., and Haberle R. M. (2012) Suppression of the water ice and snow albedo feedback on planets orbiting red dwarf stars and the subsequent widening of the habitable zone. *Astrobiology*, 12: 3-8.
- Kaltenegger L., Henning W. G., and Sasselov D. D. (2010) Detecting volcanism on extrasolar planets. *Astronom. J.*, 140: 1370-1380.
- Kaltenegger L., Traub W. A., and Jucks K. W. (2007) Spectral evolution of an Earth-like planet. *Astrophys. J.*, 658: 598-616.

- Kashefi K., and Lovley D. R. (2003) Extending the upper temperature limit for life. *Science*, 301: 934-934.
- Kaspi Y., and Showman A. P. (2015) Atmospheric dynamics of terrestrial exoplanets over a wide range of orbital and atmospheric parameters. *Astrophys. J.*, 804: 60.
- Kasting J. F. (1997) Habitable zones around low mass stars and the search for extraterrestrial life. *Origins of Life*, 27: 291-307.
- Kasting J. F. (2013) What caused the rise of atmospheric O₂? *Chem. Geol.*, 362: 13-25.
- Kasting J. F., and Catling D. (2003) Evolution of a habitable planet. *Ann. Rev. Astron. Astrophys.*, 41: 429-463.
- Kasting J. F., Holland H. D., and Pinto J. P. (1985) Oxidant abundances in rainwater and the evolution of atmospheric oxygen. *J. Geophys. Res.*, 90: 10,497-10,510.
- Kasting J. F., Pavlov A. A., and Siefert J. L. (2001) A coupled ecosystem-climate model for predicting the methane concentration in the Archean atmosphere. *Origins Life Evol. Biosph.*, 31: 271-285.
- Kasting J. F., Whitmire D. P., and Reynolds R. T. (1993) Habitable zones around main sequence stars. *Icarus*, 101: 108-128.
- Kawahara H. (2016) Frequency modulation of directly imaged exoplanets: Geometric effect as a probe of planetary obliquity. *Astrophys. J.*, 822.
- Kawahara H., and Fujii Y. (2010) Global mapping of Earth-Like exoplanets from scattered light curves. *Astrophys. J.*, 720: 1333-1350.
- Kehoe D. M., and Gutu A. (2006) Responding to color: The regulation of complementary chromatic adaptation. In: *Ann. Rev. Plant Biol.*, pp 127-150.
- Kepler F., Harper D. B., Rockmann T., Moore R. M., and Hamilton J. T. G. (2005) New insight into the atmospheric chloromethane budget gained using stable carbon isotope ratios. *Atmos. Chem. Phys.*, 5: 2403-2411.
- Kiang N. Y., Siefert J., Govindjee, and Blankenship R. E. (2007) Spectral signatures of photosynthesis I: Review of Earth organisms. *Astrobiology, Special Issue on M stars*, 7: 222-251.
- Knutson H. A., Benneke B., Deming D., and Homeier D. (2014) A featureless transmission spectrum for the Neptune-mass exoplanet GJ 436b. *Nature*, 505: 66-68.
- Koll D. D. B., and Abbot D. S. (2016) Temperature structure and atmospheric circulation of dry tidally locked rocky exoplanets. *Astrophys. J.*, 825.
- Koonin E. V. (2012) *The Logic of Chance: The Nature and Origin of Biological Evolution*. Pearson Education, Upper Saddle River, N.J.
- Kopp G., and Lean J. L. (2011) A new, lower value of total solar irradiance: Evidence and climate significance. *Geophys. Res. Lett.*, 38: L01706, doi:10.1029/2010GL045777.
- Kopparapu R. K., Ramirez R., Kasting J. F., Eymet V., Robinson T. D., Mahadevan S., Terrien R. C., Domagal-Goldman S., Meadows V., and Deshpande R. (2013) Habitable zones around main-sequence stars: New estimates. *Astrophys. J.*, 765: doi: 10.1088/0004-637X/765/2/131.
- Kopparapu R. K., Wolf E. T., Haqq-Misra J., Yang J., Kasting J. F., Meadows V., Terrien R., and Mahadevan S. (2016) The inner edge of the habitable zone for synchronously rotating planets around low-mass stars using general circulation models. *Astrophysical Journal*, 819: 84.
- Kral T. A., Brink K. M., Miller S. L., and McKay C. P. (1998) Hydrogen consumption by methanogens on the early Earth. *Origins Life Evol. Biosph.*, 28: 311-319.
- Krasnopolsky V. A. (2012) Search for methane and upper limits to ethane and SO₂ on Mars. *Icarus*, 217: 144-152.
- Kreidberg L., Bean J. L., Desert J. M., Benneke B., Deming D., Stevenson K. B., Seager S., Berta-Thompson Z., Seifahrt A., and Homeier D. (2014) Clouds in the atmosphere of the super-Earth exoplanet GJ 1214b. *Nature*, 505: 69-72.

- Krissansen-Totton J., Bergsman D. S., and Catling D. C. (2016a) On detecting biospheres from chemical thermodynamic disequilibrium in planetary atmospheres. *Astrobiology*, 16: 39-67.
- Krissansen-Totton J., and Catling D. C. (2017) Constraining climate sensitivity and continental versus seafloor weathering using an inverse geological carbon cycle model. *Nat. Commun.*: doi:10.1038/ncomms15423.
- Krissansen-Totton J., Schwieterman E. W., Charnay B., Arney G., Robinson T. D., Meadows V., and Catling D. C. (2016b) Is the Pale Blue Dot unique? Optimized photometric bands for identifying Earth-like exoplanets. *Astrophys. J.*, 817: 31.
- Kump L. R., Kasting J. F., and Crane R. G. (2010) *The Earth System*. Pearson, Upper Saddle River, NJ.
- Lada C. J. (2006) Stellar multiplicity and the initial mass function: Most stars are single. *Astrophys. J.*, 640: L63-L66.
- Lang E. W. (1986) Physical-chemical limits for the stability of biomolecules. *Adv. Space Res.*, 6: 251-255.
- Langmuir C. H., and Broecker W. S. (2012) *How to Build a Habitable Planet: The Story of Earth from the Big Bang to Humankind*. Princeton University Press, Princeton, N.J. ; Woodstock.
- Lee J. M., Heng K., and Irwin P. G. J. (2013) Atmospheric retrieval analysis of the directly imaged exoplanet HR 8799b. *Astrophys. J.*, 778: 97.
- Li Y. Q., and Chen M. (2015) Novel chlorophylls and new directions in photosynthesis research. *Funct. Plant. Biol.*, 42: 493-501.
- Line M. R., Knutson H., Wolf A. S., and Yung Y. L. (2014) A systematic retrieval analysis of secondary eclipse spectra. II. A uniform analysis of nine planets and their C to O ratios. *Astrophys. J.*, 783: 70.
- Line M. R., Wolf A. S., Zhang X., Knutson H., Kammer J. A., Ellison E., Deroo P., Crisp D., and Yung Y. L. (2013) A systematic retrieval analysis of secondary eclipse spectra. I. A Comparison of atmospheric retrieval techniques. *Astrophys. J.*, 775: 137.
- Line M. R., and Yung Y. L. (2013) A systematic retrieval analysis of secondary eclipse spectra. III. Diagnosing chemical disequilibrium in planetary atmospheres. *Astrophys. J.*, 779: 3.
- Linsky J., L. , France K., and Ayres T. (2013) Computing intrinsic LY α fluxes of F5 V to M5 V Stars. *Astrophys. J.*, 766: 69.
- Linsky J. L., and Güdel M. (2015) Exoplanet host star radiation and plasma environment. In: *Characterizing Stellar and Exoplanetary Environments*. edited by H Lammer and M Khodachenkos, Springer, Cham, Switzerland, pp 3-18.
- Livengood T. A., Deming L. D., A'Hearn M. F., Charbonneau D., Hewagama T., Lisse C. M., McFadden L. A., Meadows V. S., Robinson T. D., Seager S. and others. (2011) Properties of an Earth-like planet orbiting a sun-like star: Earth observed by the EPOXI mission. *Astrobiology*, 11: 907-930.
- Lovelock J. E. (1965) A physical basis for life detection experiments. *Nature*, 207: 568-570.
- Lovelock J. E. (1975) Thermodynamics and the recognition of alien biospheres. *Proc. Roy. Soc. Lon.*, B189: 167-181.
- Lubin P. (2016) A roadmap to interstellar flight. *J. Brit. Interplan. Soc.*, 69: 40-72.
- Luger R., and Barnes R. (2015) Extreme water loss and abiotic O₂ buildup on planets throughout the habitable zones of M dwarfs. *Astrobiology*, 15: 119-143.
- Lyons T. W., Reinhard C. T., and Planavsky N. J. (2014) The rise of oxygen in Earth's early ocean and atmosphere. *Nature*, 506: 307-315.
- Mackenzie F. T., and Lerman A. (2006) *Carbon in the Geobiosphere: Earth's Outer Shell*. Springer, Dordrecht.
- Manchester Z., and Loeb A. (2017) Stability of a light sail riding on a laser beam. *Astrophys. J. Lett.*: accepted, arXiv:1609.09506.

- Mardling R. A. (2010) The determination of planetary structure in tidally relaxed inclined systems. *Mon. Not. R. Astron. Soc.*, 407: 1048-1069.
- Marley M. S., Ackerman A. S., Cuzzi J. N., and Kitzmann D. (2013) Clouds and hazes in exoplanets. In: *Comparative Climatology of Terrestrial Planets*. edited by SJ Mackwell, AA Simon-Miller, JW Harder and MA Bullocks, Univ. of Arizona Press, Tucson, pp 367-391.
- Marosvolgyi M. A., and van Gorkom H. J. (2010) Cost and color of photosynthesis. *Photosyn. Res.*, 103: 105-109.
- McCollom T. M. (2016) Abiotic methane formation during experimental serpentinization of olivine. *P. Natl. Acad. Sci. USA*, 113: 13965-13970.
- McCollom T. M., and Donaldson C. (2016) Generation of hydrogen and methane during experimental low-temperature reaction of ultramafic rocks with water. *Astrobiology*, 16: 389-406.
- Meadows V. S. (2017) Reflections on O₂ as a biosignature in exoplanetary atmospheres. *Astrobiology*: doi:10.1089/ast.2016.1578.
- Meadows V. S., and co-authors. (2017) Exoplanet biosignatures: Understanding oxygen as a biosignature in the context of Its environment. *Astrobiol.*: this issue.
- Milo R. (2009) What governs the reaction center excitation wavelength of photosystems I and II? *Photosyn. Res.*, 101: 59-67.
- Misra A., Krissansen-Totton J., Koehler M. C., and Sholes S. (2015) Transient sulfate aerosols as a signature of exoplanet volcanism. *Astrobiology*, 15: 462-477.
- Misra A., Meadows V., Claire M., and Crisp D. (2014) Using dimers to measure biosignatures and atmospheric pressure for terrestrial exoplanets. *Astrobiology*, 14: 67-86.
- Monod J. (1971) *Chance and Necessity: An essay on the Natural Philosophy of Modern Biology*. Knopf, New York.
- Moran J. J., House C. H., Vrentas J. M., and Freeman K. H. (2008) Methyl sulfide production by a novel carbon monoxide metabolism in *Methanosarcina acetivorans*. *Appl. Environ. Microbiol.*, 74: 540-542.
- Moriarty J., Madhusudhan N., and Fischer D. (2014) Chemistry in an evolving protoplanetary disk: Effects on terrestrial planet composition. *Astrophys. J.*, 787: 81.
- Moroz V. I., Ekonomov A. P., Moshkin B. E., Revercomb H. E., Sromovsky L. A., Schofield J. T., Spänkuch D., Taylor F. W., and Tomasko M. G. (1985) Solar and thermal radiation in the Venus atmosphere. *Adv. Space Res.*, 5: 197-232.
- Myneni R. B., Maggion S., Iaquina J., Privette J. L., Gobron N., Pinty B., Kimes D. S., Verstraete M. M., and Williams D. L. (1995) Optical remote sensing of vegetation: modeling, caveats, and algorithms. *Remote Sens. Environ.*, 51: 169-188.
- Myneni R. B., Nemani R. R., and Running S. W. (1997) Estimation of global leaf area index and absorbed PAR using radiative transfer models. *IEEE Trans. Geosci. Remote Sens.*, 35: 1380-1393.
- Oakley P. H. H., and Cash W. (2009) Construction of an Earth model: Analysis of exoplanet light curves and mapping the next Earth with the New Worlds Observer. *Astrophys. J.*, 700: 1428-1439.
- Oklopčić A., Hirata C. M., and Heng K. (2016) Raman scattering by molecular hydrogen and nitrogen in exoplanetary atmospheres. *Astrophys. J.*, 832.
- Owen T. (1980) The search for early forms of life in other planetary systems: future possibilities afforded by spectroscopic techniques. In: *Strategies for Search for Life in the Universe*. edited by MD Papagianniss, Reidel, Dordrecht, pp 177-185.
- Owen T. C., and Kuiper G. P. (1964) A determination of the composition and surface pressure of the Martian atmosphere. *Commun. Lunar Planet. Lab.*, 32: 113-132.

- Pallavicini R., Golub L., Rosner R., Vaiana G. S., Ayres T., and Linsky J. L. (1981) Relations among stellar x-ray-emission observed from Einstein, stellar rotation and bolometric luminosity. *Astrophysical Journal*, 248: 279-290.
- Palle E., Ford E. B., Seager S., Montanes-Rodriguez P., and Vazquez M. (2008) Identifying the rotation rate and the presence of dynamic weather on extrasolar earth-like planets from photometric observations. *Astrophys. J.*, 676: 1319-1329.
- Palle E., Goode P. R., Yurchyshyn V., Qiu J., Hickey J., Rodriguez P. M., Chu M. C., Kolbe E., Brown C. T., and Koonin S. E. (2003) Earthshine and the Earth's albedo: 2. Observations and simulations over 3 years. *J. Geophys. Res.*, 108: 4710, doi:10.1029/2003jd003611.
- Palmer K. F., and Williams D. (1975) Optical constants of sulfuric acid: Application to the clouds of Venus? *Appl. Opt.*, 14: 208-219.
- Parenteau M. N., Kiang N. Y., Blankenship R. E., Sanromá E., Pallé E., Hoehler T. M., Pierson B. K., and Meadows V. S. (2015) Remotely detectable biosignatures of anoxygenic phototrophs. In: *Astrobiol. Sci. Conf.*, Chicago, IL.
- Pierrehumbert R., and Gaidos E. (2011) Hydrogen greenhouse planets beyond the habitable zone. *Astrophys. J. Lett.*, 734.
- Pierrehumbert R. T. (2010) Principles of Planetary Climate. Cambridge Univ. Press, Cambridge.
- Pleskot L. K., and Miner E. D. (1981) Time variability of martian bolometric albedo. *Icarus*, 45: 179-201.
- Pollack J. B., Strecker D. W., Witteborn F. C., Erickson E. F., and Baldwin B. J. (1978) Properties of the clouds of Venus, as inferred from airborne observations of its near-infrared reflectivity spectrum. *Icarus*, 34: 28-45.
- Qiu J., Goode P. R., Palle E., Yurchyshyn V., Hickey J., Rodriguez P. M., Chu M. C., Kolbe E., Brown C. T., and Koonin S. E. (2003) Earthshine and the Earth's albedo: 1. Earthshine observations and measurements of the lunar phase function for accurate measurements of the Earth's Bond albedo. *Journal of Geophysical Research-Atmospheres*, 108.
- Ragsdale S. W. (2004) Life with carbon monoxide. *Crit. Rev. Biochem. Mol.*, 39: 165-195.
- Rauscher E., and Kempton E. M. R. (2014) The atmospheric circulation and observable properties of non-synchronously rotating hot jupiters. *Astrophys. J.*, 790: 79.
- Raven J. A., Giordano M., Beardall J., and Maberly S. C. (2012) Algal evolution in relation to atmospheric CO₂: Carboxylases, carbon-concentrating mechanisms and carbon oxidation cycles. *Phil Trans. Roy. Soc. Lond. B*, 367: 493-507.
- Rea D. G., O'Leary B. T., and Sinton W. M. (1965) Mars: Origin of 3.58- and 3.69-micron minima in infrared spectra. *Science*, 147: 1286-&.
- Rein H., Fujii Y., and Spiegel D. S. (2014) Some inconvenient truths about biosignatures involving two chemical species on Earth-like exoplanets. *P. Natl. Acad. Sci. USA*, 111: 6871-6875.
- Reynolds R. T., McKay C. P., and Kasting J. F. (1987) Europa, tidally heated oceans, and habitable zones around giant planets. *Adv. Space Res.*, 7: 125-132.
- Ribas I., Guinan E. F., Gudel M., and Audard M. (2005) Evolution of the solar activity over time and effects on planetary atmospheres. I. High-energy irradiances (1-1700 angstrom). *Astrophys. J.*, 622: 680-694.
- Robinson T. D. (2017) Characterizing exoplanets for habitability. In: *Handbook of Exoplanets*. edited by H Deeg and JA Belmontes, Springer, New York, pp arXiv:1701.05205.
- Robinson T. D., Maltagliati L., Marley M. S., and Fortney J. J. (2014) Titan solar occultation observations reveal transit spectra of a hazy world. *P. Natl. Acad. Sci. USA*, 111: 9042-9047.
- Robinson T. D., Meadows V. S., and Crisp D. (2010) Detecting oceans on extrasolar planets using the glint effect. *Astrophys. J. Lett.*, 721: L67-L71.
- Robinson T. D., Meadows V. S., Crisp D., Deming D., A'Hearn M. F., Charbonneau D., Livengood T. A., Seager S., Barry R. K., Hearty T. and others. (2011) Earth as an extrasolar planet: Earth model validation using EPOXI Earth observations. *Astrobiology*, 11: 393-408.

- Rocchetto M., Waldmann I. P., Venot O., Lagage P. O., and Tinetti G. (2016) Exploring biases of atmospheric retrievals in simulated JWST transmission spectra of Hot Jupiters. *Astrophys. J.*, 833: 120.
- Rodgers C. D. (2000) *Inverse Methods for Atmospheric Sounding: Theory and Practice*. World Scientific, River Edge, NJ.
- Rozelot J. P., and Neiner C. (2009) *The Rotation of Sun and Stars*. Springer, Berlin, pp 263.
- Rubasinghe G., Spak S. N., Stanier C. O., Carmichael G. R., and Grassian V. H. (2011) Abiotic mechanism for the formation of atmospheric nitrous oxide from ammonium nitrate. *Environ. Sci. & Tech.*, 45: 2691-2697.
- Rugheimer S., Kaltenegger L., Segura A., Linsky J., and Mohanty S. (2015) Effect of UV radiation on the spectral fingerprints of Earth-Like planets orbiting M stars. *Astrophys. J.*, 809: 57.
- Rugheimer S., Kaltenegger L., Zsom A., Segura A., and Sasselov D. (2013) Spectral fingerprints of Earth-like planets around FGK stars. *Astrobiology*, 13: 251-269.
- Rushby A. J., Claire M. W., Osborn H., and Watson A. J. (2013) Habitable Zone Lifetimes of Exoplanets around Main Sequence Stars. *Astrobiology*, 13: 833-849.
- Sagan C. (1994) *Pale Blue Dot: A vision of the human future in space*. Random House, New York.
- Sagan C., and Chyba C. (1997) The early faint Sun paradox: Organic shielding of ultraviolet-labile greenhouse gases. *Science*, 276: 1217-1221.
- Sagan C., and Mullen G. (1972) Earth and Mars: Evolution of atmospheres and surface temperatures. *Science*, 177: 52-56.
- Sagan C., Thompson W. R., Carlson R., Gurnett D., and Hord C. (1993) A search for life on Earth from the Galileo spacecraft. *Nature*, 365: 715-721.
- Samarkin V. A., Madigan M. T., Bowles M. W., Casciotti K. L., Priscu J. C., Mckay C. P., and Joye S. B. (2010) Abiotic nitrous oxide emission from the hypersaline Don Juan Pond in Antarctica. *Nature Geoscience*, 3: 341-344.
- Scharf C., and Cronin L. (2016) Quantifying the origins of life on a planetary scale. *P. Natl. Acad. Sci. USA*, 113: 8127-8132.
- Schmidt G. A., Ruedy R. A., Miller R. L., and Lacis A. A. (2010) Attribution of the present-day total greenhouse effect. *J. Geophys. Res.*, 115: D20106, doi:10.1029/2010JD014287.
- Schwieterman E. W., Meadows V. S., Domagal-Goldman S. D., Deming D., Arney G. N., Luger R., Harman C. E., Misra A., and Barnes R. (2016) Identifying planetary biosignature impostors: Spectral features of CO and O₄ resulting from abiotic O₂/O₃ production. *Astrophys. J. Lett.*, 819: L13.
- Schwieterman E. W., Cockell C. S., and Meadows V. S. (2015a) Nonphotosynthetic pigments as potential biosignatures. *Astrobiology*, 15: 341-361.
- Schwieterman E. W., Kiang N. Y., Parenteau M. N., Harman C. E., DasSarma S., Fisher T. M., Arney G. N., Hartnett H. E., Reinhard C. T., Olson S. L. and others. (2017) Exoplanet biosignatures: A review of remotely detectable signs of life. *Astrobiol.*: this issue, arXiv:1705.05791.
- Schwieterman E. W., Robinson T. D., Meadows V. S., Misra A., and Domagal-Goldman S. (2015b) Detecting and constraining N₂ abundances in planetary atmospheres using collisional pairs. *Astrophys. J.*, 810: 57.
- Seager S. (2013) Exoplanet habitability. *Science*, 340: 577-581.
- Seager S., and Bains W. (2015) The search for signs of life on exoplanets at the interface of chemistry and planetary science. *Science Advances*, 1: <http://dx.doi.org/10.1126/sciadv.1500047>.
- Seager S., Turner E. L., Schafer J., and Ford E. B. (2005) Vegetation's red edge: a possible spectroscopic biosignature of extraterrestrial plants. *Astrobiology*, 5: 372-390.
- Segura A., Kasting J. F., Meadows V., Cohen M., Scalo J., Crisp D., Butler R. A. H., and Tinetti G. (2005) Biosignatures from earth-like planets around M dwarfs. *Astrobiology*, 5: 706-725.

- Segura A., Krelow K., Kasting J. F., Sommerlatt D., Meadows V., Crisp D., Cohen M., and Mlawer E. (2003) Ozone concentrations and ultraviolet fluxes on Earth-like planets around other stars. *Astrobiology*, 3: 689-708.
- Shields A. L., Meadows V. S., Bitz C. M., Pierrehumbert R. T., Joshi M. M., and Robinson T. D. (2013) The effect of host star spectral energy distribution and ice-albedo feedback on the climate of extrasolar planets. *Astrobiology*, 13: 715-739.
- Shklovskii I. S., and Sagan C. (1966) *Intelligent Life in the Universe*. Holden-Day, San Francisco, CA.
- Sholes S. F., Smith M. L., Claire M. W., Zahnle K. J., and Catling D. C. (2017) Anoxic atmospheres on early Mars driven by volcanism: Implications for past environments and life. *Icarus*, 290: 46-52.
- Showman A. P., Wordsworth R. D., Merlis T. M., and Kaspi Y. (2013) Atmospheric circulation of terrestrial exoplanets. In: *Comparative Climatology of Terrestrial Planets*. edited by SJ Mackwell, AA Simon-Miller, JW Harder and MA Bullocks, Univ. of Arizona Press, Tucson, pp 277-326.
- Sinton W. M. (1957) Spectroscopic evidence for vegetation on Mars. *Astrophys. J.*, 126: 231-239.
- Sinton W. M. (1959) Further evidence of vegetation on Mars. *Science*, 130: 1234-1237.
- Sinukoff E., Howard A. W., Petigura E. A., Schlieder J. E., Crossfield I. J. M., Ciardi D. R., Fulton B. J., Isaacson H., Aller K. M., Baranec C. and others. (2016) Eleven multiplanet systems from K2 campaigns 1 and 2 and the masses of two hot Super-Earths. *Astrophys. J.*, 827: 78.
- Slettebak A. (1985) Determination of stellar rotational velocities. In: *Calibration of Fundamental Stellar Quantities: Proceedings of the 111th Symposium of the IAU*. edited by DS Hayes, LE Pasinetti and AGD Philips, D. Reidel, Boston, pp 163-183.
- Slonczewski J. L., Coker J. A., and DasSarma S. (2010) Microbial growth with multiple stressors. *Microbe*, 5: 110-116.
- Smith E., and Morowitz H. J. (2016) *The Origin and Nature of Life on Earth: The Emergence of the Fourth Geosphere*. Cambridge University Press, New York, NY.
- Soderblom J. M., Barnes J. W., Soderblom L. A., Brown R. H., Griffith C. A., Nicholson P. D., Stephan K., Jaumann R., Sotin C., Baines K. H. and others. (2012) Modeling specular reflections from hydrocarbon lakes on Titan. *Icarus*, 220: 744-751.
- Somero G. N. (1995) Proteins and temperature. *Annu. Rev. Physiol.*, 57: 43-68.
- Sparks W., Hough J. H., Germer T. A., Robb F., and Kolokolova L. (2012) Remote sensing of chiral signatures on Mars. *Planet. Space Sci.*, 72: 111-115.
- Sparks W. B., Hough J., Germer T. A., Chen F., DasSarma S., DasSarma P., Robb F. T., Manset N., Kolokolova L., Reid N. and others. (2009) Detection of circular polarization in light scattered from photosynthetic microbes. *P. Natl. Acad. Sci. USA*, 106: 7816-7821.
- Spiegel D., S. , Haiman Z., and Gaudi B. S. (2007) On constraining a transiting exoplanet's rotation rate with its transit spectrum. *Astrophys. J.*, 669: 1324.
- Spiegel D. S., and Turner E. L. (2012) Bayesian analysis of the astrobiological implications of life's early emergence on Earth. *P. Natl. Acad. Sci. USA*, 109: 395-400.
- Stam D. M. (2008) Spectropolarimetric signatures of Earth-like extrasolar planets. *Astronomy & Astrophysics*, 482: 989-1007.
- Stephan K., Jaumann R., Brown R. H., Soderblom J. M., Soderblom L. A., Barnes J. W., Sotin C., Griffith C. A., Kirk R. L., Baines K. H. and others. (2010) Specular reflection on Titan: Liquids in Kraken Mare. *Geophysical Research Letters*, 37.
- Stephens G. L., O'Brien D., Webster P. J., Pilewski P., Kato S., and Li J.-l. (2015) The albedo of Earth. *Rev. Geophys.*, 53: 141-163.
- Stevenson D. J. (1999) Life-sustaining planets in interstellar space? *Nature*, 400: 32-32.

- Stocker T. F., Qin D., Plattner G.-K., Tignor M., Allen S. K., Boschung J., Nauels A., Xia Y., Bex V., and Midgley P. M. (2013) IPCC, 2013: Climate Change: The Physical Science Basis. Cambridge Univ. Press, New York, NY.
- Stomp M., Huisman J., Vörös L., Pick F. R., Laamanen M., Thomas, Haverkamp, and Stal L. J. (2007) Colourful coexistence of red and green picocyanobacteria in lakes and seas. *Ecology Letters*, 10: 290-298.
- Stone J. V. (2013) Bayes' Rule: A Tutorial Introduction to Bayesian Analysis. Sebtel Press, Sheffield, UK.
- Tian B., and Hua Y. J. (2010) Carotenoid biosynthesis in extremophilic *Deinococcus-Thermus* bacteria. *Trends Microbiol.*, 18: 512-520.
- Tian F., France K., Linsky J. L., Mauas P. J. D., and Vieytes M. C. (2014) High stellar FUV/NUV ratio and oxygen contents in the atmospheres of potentially habitable planets. *Earth Planet. Sc. Lett.*, 385: 22-27.
- Titov D. V., Piccioni G., Drossart P., and Markiewicz W. J. (2013) Radiative energy balance in the Venus atmosphere. In: *Towards Understanding the Climate of Venus*. edited by L Bengtsson, R-M Bonnet, D Grinspoon, S Koumoutsaris, S Lebonnois and D Titovs, Springer, New York, pp 23-53.
- Trainer M. G., Pavlov A. A., DeWitt H. L., Jimenez J. L., McKay C. P., Toon O. B., and Tolbert M. A. (2006) Organic haze on Titan and the early Earth. *P. Natl. Acad. Sci. USA*, 103: 18035-18042.
- Tucker C. J., Pinzon J. E., Brown M. E., Slayback D. A., Pak E. W., Mahoney R., Vermote E. F., and El Saleous N. (2005) An extended AVHRR 8-km NDVI dataset compatible with MODIS and SPOT vegetation NDVI data. *Int. J. Remote Sens.*, 26: 4485-4498.
- Twomey S. (1996) Introduction to the Mathematics of Inversion in Remote Sensing and Indirect Measurements. Dover Publications, Inc., Mineola, NY.
- van Belle G. T. (2012) Interferometric observations of rapidly rotating stars. *Astron. Astrophys. Rev.*, 20: 51.
- Waite J. H., Glein C. R., Perryman R. S., Teolis B. D., Magee B. A., Miller G., Grimes J., Perry M. E., Miller K. E., Bouquet A. and others. (2017) Cassini finds molecular hydrogen in the Enceladus plume: Evidence for hydrothermal processes. *Science*, 356: 155-159.
- Waldmann I. P., Rocchetto M., Tinetti G., Barton E. J., Yurchenko S. N., and Tennyson J. (2015) Tau-REx II: Retrieval of emission spectra. *Astrophys. J.*, 813: 13.
- Walker J. C. G., Hays P. B., and Kasting J. F. (1981) A negative feedback mechanism for the long-term stabilization of Earth's surface temperature. *J. Geophys. Res.*, 86: 9776-9782.
- Walker S. I. (2017) Origins of life: A problem for physics. *Rep. Prog. Phys.*: submitted.
- Walker S. I., and co-authors. (2017) Exoplanet Biosignatures: Future Directions. *Astrobiol.*: this issue.
- Wang J., and Fischer D. A. (2015) Revealing a universal planet-metallicity correlation for planets of different solar-type stars. *Astron. J.*, 149.
- Wang Y. W., Tian F., Li T., and Hu Y. Y. (2016) On the detection of carbon monoxide as an anti-biosignature in exoplanetary atmospheres. *Icarus*, 266: 15-23.
- Warren S. G., and Brandt R. E. (2008) Optical constants of ice from the ultraviolet to the microwave: A revised compilation. *J. Geophys. Res.*, 113: D14220, doi:10.1029/2007JD009744.
- Way M. J., Del Genio A. D., Kiang N. Y., Sohl L. E., Grinspoon D. H., Aleinov I., Kelley M., and Clune T. (2016) Was Venus the first habitable world of our solar system? *Geophys. Res. Lett.*, 43: 8376-8383.
- Weiss M. C., Sousa F. L., Mrnjavac N., Neukirchen S., Roettger M., Nelson-Sathi S., and Martin W. F. (2016) The physiology and habitat of the last universal common ancestor. *Nature Microbiology*, 1: 16116 doi:10.1038/nmicrobiol.2016.116.
- White R. H. (1984) Hydrolytic stability of biomolecules at high-temperatures and its implication for life at 250°C. *Nature*, 310: 430-432.

- Williams D. M., and Gaidos E. (2008) Detecting the glint of starlight on the oceans of distant planets. *Icarus*, 195: 927-937.
- Williams D. M., Kasting J. F., and Caldeira K. (1996) Chaotic obliquity variations and planetary habitability. In: *Circumstellar Habitable Zones*. edited by LR Doyles, Travis House Publications, Menlo Park, CA, pp 43-62.
- Williams D. M., and Pollard D. (2002) Earth-like worlds on eccentric orbits: excursions beyond the habitable zone. *Int. J. Astrobiol.*, 1: 61-69.
- Wordsworth R., and Pierrehumbert R. (2014) Abiotic oxygen-dominated atmospheres on terrestrial habitable zone planets. *Astrophys. J. Lett.*, 785: L20.
- Wozniak B., and Dera J. (2007) Light Absorption in Sea Water. Springer, New York, NY.
- Yang J., Boué G., Fabrycky D., C. , and Abbot D. S. (2014) Strong dependence of the inner edge of the habitable zone on planetary rotation rate. *Astrophys. J. Lett.*, 787: L2.
- Yao Y., and Giapis K. P. (2017) Dynamic molecular oxygen production in cometary comae. *Nat. Commun.*, 8: 15298, doi:10.1038/ncomms15298.
- Zahnle K., Haberle R. M., Catling D. C., and Kasting J. F. (2008) Photochemical instability of the ancient Martian atmosphere. *J. Geophys. Res.*, 113: E11004.
- Zahnle K., Schaefer L., and Fegley B. (2010) Earth's earliest atmospheres. *CSH Perspect. Biol.*, 2: doi: 10.1101/cshperspect.a004895.
- Zahnle K. J., and Catling D. C. (2014) Waiting for oxygen. In: *Special Paper 504: Early Earth's Atmosphere and Surface Environment*. edited by GH Shaws, Geological Soc. of America, Boulder, CO, pp 37-48.
- Zahnle K. J., and Catling D. C. (2017) The cosmic shoreline: The evidence that escape determines which planets have atmospheres, and what this may mean for Proxima Centauri b. *Astrophys. J.*: in revision (<https://arxiv.org/abs/1702.03386>).
- Zhang X., and Showman A. P. (2017) Effects of bulk composition on the atmospheric dynamics on close-in exoplanets. *Astrophys. J.*, 836: 73.
- Zsom A. (2015) A population-based habitable zone perspective. *Astrophys. J.*, 813: 9.
- Zugger M. E., Kasting J. F., Williams D. M., Kane T. J., and Philbrick C. R. (2010) Light scattering from exoplanet oceans and atmospheres. *Astrophys. J.*, 723: 1168-1179.